Chair of Processing of Composites

Doctoral Thesis

Pultrusion of thermoset based profiles-state of the art regarding materials, process set-ups, process modeling, and process simulation

Rita de Cassia Costa Dias

February 2020

AFFIDAVIT

I declare on oath that I wrote this thesis independently, did not use other than the specified sources and aids, and did not otherwise use any unauthorized aids.

I declare that I have read, understood, and complied with the guidelines of the senate of the Montanuniversität Leoben for "Good Scientific Practice".

Furthermore, I declare that the electronic and printed version of the submitted thesis are identical, both, formally and with regard to content.

Date 20.02.2020

Signature Author
Rita de Cássia, Costa Dias

To the memory of my beloved father Jose Isidorio Dias

Acknowledgement

This PhD work at Montanuniversitt Leoben is funded by the Coordenação de Aperfeiçoamento de Pessoal de Nível Superior (CAPES) - Brazil, which is kindly acknowledged.

First and foremost I would like to express my deepest appreciation to my main supervisor Professor Ralf Schledjewski for his supervision and I would like to express my sincere thanks to the partner this work, Professor Lizandro de Sousa Santos for his continued support and guidance from beginning to end of my PhD work. I would like to thanks to the Dr. Hacène Ouzia for welcoming me to the Université Pierre et Marie Curie for 6 months and helping me with all the early part of my numerical optimization work.

I thank the Assistant Professor Ewald Fauster for his help to all experimental work on the characterization of the material studied and experiments on Pultrusion line. I thank the lab technicians, the department secretaries, and my colleagues who always helped me and especially my dear friend Silvia Loret Pertegás.

I would like to dedicate this thesis to the memory of my beloved father José Isidorio Dias (meu Chu) whose role in my life was, and remains, immense.

I thank also to my mother (minha Popis), who always believed in my dreams and let me fly.

Abstract

This thesis focuses on mathematical modeling of the pultrusion process in order to improve the degree of cure and thermal arrangement during the polymerization reaction. The main focus is on the use of thermo-chemical and empirical kinetic models for the prediction of the degree of cure. While empirical kinetic models are easy to handle, they are limited in terms of providing it with an understanding of the system due to the absence of knowledge regarding the full kinetic of the functional groups. In this regard, the use of phenomenological models, based on material scales of functional groups involved in the curing reaction, is a noteworthy strategy. The kinetic parameters of both models were estimated from differential scanning calorimetry (DSC) experiments of an epoxy resin. Results of parameter estimation, by comparison with experimental data, revealed that the kinetic models could be reasonably adjusted to the experimental cure behavior, presenting a small mean squared deviation. In the pultrusion process, there are many amount of variables involved and this includes the pull speed and die temperature. Thus, the dedication to the study of computational models is required in order to analyze the process for different composite manufacturing aspects such as heat transfer, curing properties in order to obtain good quality over the mechanical properties of the pultruded material. In addition to the scientific and thermochemical models developed in this thesis, we observed that few studies have been focusing on matrix temperature optimization of the pultrusion process. This work also aims to optimize the die-temperature of pultrusion based on minimizing the objective function by varying the values of the temperatures of die heaters, which are the decision variables of optimization problem. This work show the mean of the cure degree is satisfactory when used with many internal heaters and the results indicate that the algorithm used in this study is numerically reliable and provides optimal die temperatures for providing uniformly cured material.

Kurzzusammenfassung

Diese Arbeit widmet sich der mathematischen Modellierung des Pultrusionsprozesses, um den Härtungsgrad und die Wärmeverteilung während der Polymerisationsreaktion zu verbessern. Das Hauptaugenmerk liegt auf der Verwendung thermochemischer und empirischer kinetischer Modelle zur Vorhersage des Aushärtegrades. Während empirische kinetische Modelle einfach zu handhaben sind, sind sie hinsichtlich des Verständnisses des Systems begrenzt, da kein Wissen über die vollständige Kinetik der funktionellen Gruppen vorliegt. In dieser Hinsicht ist die Verwendung von phänomenologischen Modellen, die auf Materialskalen der an der Härtungsreaktion beteiligten funktionellen Gruppen basieren, eine gute Strategie. Die kinetischen Parameter beider Modelle wurden aus Differential Scanning Calorimetry (DSC) -Experimenten eines Epoxidharzes abgeschätzt. Die Ergebnisse der Parameterschätzung durch Vergleich mit experimentellen Daten zeigten, dass die kinetischen Modelle angemessen an das experimentelle Aushärtungsverhalten angepasst werden konnten und minimale Fehlerquadrate aufwiesen. Angesichts der Multiphysik und der Vielzahl von Variablen, die am Pultrusionsprozess beteiligt sind, sind einige experimentelle Analysen für die Herstellung zeitaufwändig. Daher ist die Entwicklung geeigneter Rechenmodelle von großem Interesse, um den Prozess auf verschiedene Aspekte der Verbundherstellung wie Wärmeübertragung, Aushärtung und mechanische Eigenschaften hin zu analysieren. Zusätzlich zu den wissenschaftlichen und thermochemischen Modellen, die in dieser Arbeit entwickelt wurden, haben wir beobachtet, dass sich nur wenige Studien mit der Optimierung der Matrixtemperatur des Pultrusionsprozesses befasst haben. Daher ist das zweite Ziel dieser Arbeit die Optimierung der Werkzeugtemperatur der Pultrusion auf der Grundlage der Minimierung der Zielfunktion durch Variieren der Werte der Temperaturen der Düsenheizungen, die die Entscheidungsvariablen des Optimierungsproblems sind. Die Ergebnisse zeigten, dass der entwickelte Algorithmus numerisch stabil ist und optimale Werkzeugtemperaturen zur Herstellung eines gleichmäßig ausgehärteten Materials bietet.

Content

Permission for Reuse of Published Content..... 8

List of Abbreviations..... 9

List of Symbols..... 10

1 Introduction and Aims 1

1.1 Polymer Composites: A Brief Introduction..... 1

1.2 Pultrusion 2

1.3. Purpose of Thesis 3

2 State of the Art 5

2.1 Brief Introduction to Polymeric Composite Pultrusion..... 5

2.1.1. Material supply..... 7

2.1.2. Profile geometries - Pultrusion die 10

2.1.3. Pulling force and Cutting machine 12

2.2. Commercial products and apllications..... 14

2.3. A brief study of thermoset resin..... 15

2.4. A study for modelling the thermosetting resin. 19

2.5. Numerical simulation..... 20

2.6. Computational fluid dynamics (CFD)..... 21

2.7. Finite volume numerical method 23

2.8. Pultrusion Die – Mathematical model. 24

2.9. FE-Nodal control volume- Optimization..... 25

2.10. Particle Swarm Algorithm (PSO)..... 26

2.11. Algorithm (QP) - quadratic programming algorithm..... 27

2.12. Empirical kinetic model 28
2.13. Phenomenological kinetic model..... 29

3 Methodology – Numerical optimization (Pultrusion die). 34
3.1 Procedure – Optimization Steps..... 34
3.2 Simulation Steps 37

4 Case Studies – Simulation of pultrusion process. 38
4.1 Case study (Validation case)..... 38
4.2. Results (Validation Case)..... 39
4.3. Results Case Study 2 (C-section) 40
4.4. Case study 3 (Internal Heaters) 41
4.5. Results (Internal Heaters) 42

5. Methodology (Kinetic Model) 47
5.1. Experimental procedure 47
5.2. Parameter estimation of empirical model 47
5.3. Parameter estimation: Optimization 48
5.4. Phenomenological kinetic model..... 49
5.5. Methodology - Flowchart..... 54

6. DSC analysis and Parameter estimation of empirical kinetic model parameterstion 56
6.1. Results of DSC analysis..... 56
6.2. Parameter estimation of empirical kinetic model parameters..... 58
6.3. Results: Parameter estimation with the phenomenological model 64
6.4. Results: Simulation of Pultrusion process 65

7. Conclusions..... 69

8. References 71

9. Appendix 77

Permission for Reuse of Published Content

This dissertation is based on the publications listed below. These publications are essential elements and represent central parts of this thesis.

Journal of Materials Science Forum

Dias, R.D.C.; Santos, L.S.; Schledjewski, R.: Comparative Study of Optimization in Pultrusion with Pre-Heating and Die-Cooler Temperature for Improved Cure. Materials Science Forum, 879, pp. 402-407, 2017,
DOI: 10.4028/www.scientific.net/MSF.879.402.

Journal of Materials Today Communications

Dias, R.D.C.; Santos, L.S.; Ouzia, H.; Schledjewski, R.: Improving degree of cure in pultrusion process by optimizing die temperature. Materials Today Communications, 17, pp. 362-370, 2018, DOI: 10.1016/j.mtcomm.2018.08.017.

Work in Progress

Journal of Thermochimica Acta

Dias, R.D.C.; Santos, L.S.; Costa, M.L.; Schledjewski, R.: Kinetic parameter estimation and simulation of pultrusion process of an epoxy-glass fiber system (Submitted - Revision Requested).

Conference Proceedings and Presentations

Dias, R.D.C.; Santos, L.S.; Schledjewski, R.: Optimization to improve the stability of finite-volume methods on unstructured meshes on simulation of pultrusion process, In: Euromech 602 colloquium, Lyon, France, 13 – 15th March, 2019.

Dias, R.D.C.; Santos, L.S.; Schledjewski, R.: Improved cure simulation in pultrusion process about heating systems: A case study, In: 17th European conference on composite materials ECCM17, Munich, Germany, 26 – 30th June, 2016.

Dias, R.D.C.; Santos, L.S.; Ouzia, H.; Schledjewski, R.: Optimization of dietemperature in pultrusion of thermosetting composites for improved cure, In: International Conference on Swarm Intelligence Based Optimization – Theoretical advances and real world application, Mulhouse, France, 13 – 14th June, 2016.

List of Abbreviations

Abbreviation	Description
CFD	Computational fluid dynamics
DSC	Differential Scanning Calorimetry
FE	Finite - element
FEM	Finite Element Method
FE/NVC	Finite Element with Nodal Control Volume
FDM	Finite Difference Method
FVM	Finite Volume Method
FRP	Fiber Reinforced Plastic
HDPE	High-density polyethylene
ODE	Ordinary differential equation
PSO	Particle Swarm Optimization
QP	Quadratic Programming algorithm
RIP	Reactive injection Pultrusion

List of Symbols

Symbol	Description	Unit
α	Degree of cure	
α_g	Degree of cure at gelation	
A	Pre-exponential factor of the Arrhenius equation	s^{-1}
$c_{p,r}$	Resin specific heat	$J.kg\text{-}1.K^{-1}$
$C_{a,0}$	Feed resin mass concentration	$kg^{-1}.K^{-1}$
$c_{p,f}$	Fiber specific heat	$J.kg.m^{-3}$
E_a	Activation energy of the Arrhenius equation	J/mol
H_R	Total heat of reaction	J/kg
m,n	Order of reaction	
K_{cat}	Autocatalytic factor	
kc	Kozeny-Carman constant	
η	Fluid apparent or dynamic Viscosity	Pa·s
P	Pressure	Pa
V_a	Maximum theoretical fiber volume fraction	
v	Flow velocity vector	m/s
K	Permeability of the porous medium	m^2
∅	Porosity	
∇P	Pressure gradient	Pa
T	Temperature	K or °C
V_f	Fiber volume content	
ρ	Density	kg/m^3

λ	Thermal conductivity	W/(m·K)
αv	Volumetric coefficient of thermal expansion	K^{-1}
β	Coefficient of volumetric shrinkage of resin due to curing	
Φ_r	Resin volume fraction	
Φ_f	Fiber volume fraction	
ρ_r	Resin density	$kg.m^{-3}$
ρ_f	Fiber specific heat	$kg.m^{-3}$
k_r	Resin thermal conductivity	$J.m^{-1}.s^{-1}$
k_f	Fiber thermal conductivity	$J.m^{-1}.s^{-1}$
r_a	Reaction rate	
R	Universal gas constant	$J \cdot kg^{-1}.K^{-1}$
w	Pulling speed	m/s

1 Introduction and Aims

1.1 Polymer Composites: A Brief Introduction

In a very broad context, composites can be divided into natural and synthetic. Among the synthetic composites, and considering the different classes related to the various matrix options, one can enumerate a number of other classifications resulting from the types and arrangements of the existing reinforcements, as shown diagrammatically in (Fig. 1) [1].

Over the last few years the use of polymer composites has been showing strong growth due to several structural advantages such as low density, structural flexibility, corrosion resistance, thermal stability and low manufacturing cost when compared to traditional materials such as aluminum and wood.

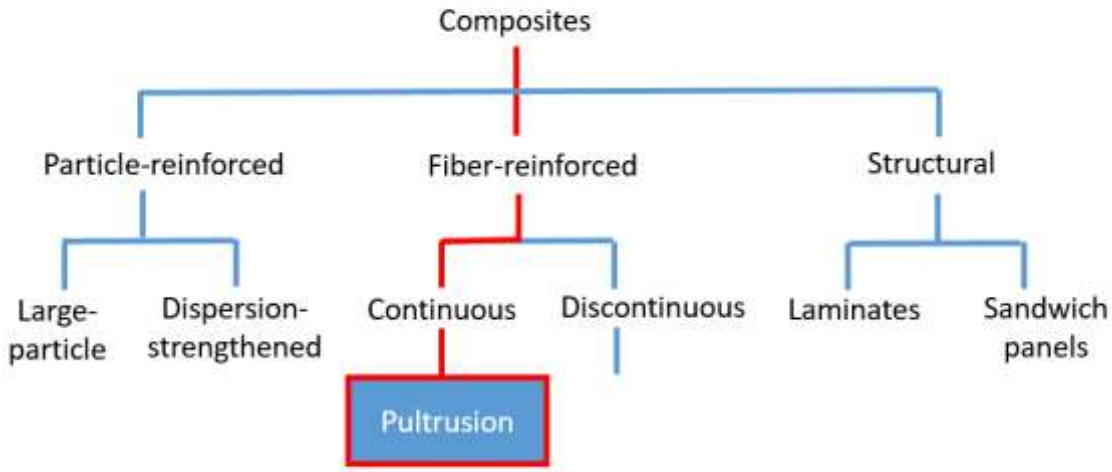

Fig. 1. Composites classification (adapted) [1].

1.2 Pultrusion

Over the last few years the use of polymer composites has been showing strong growth due to several structural advantages such as low density, structural flexibility, corrosion resistance, thermal stability and low manufacturing cost when compared to traditional materials such as aluminum and wood. Innovations in composites have allowed significant weight reduction structural projects, making them structurally more efficient projects [1, 2] One of the main factors responsible for the growing use of these materials was the development of modern manufacturing processes as well as the pultrusion process due to the fact that it is one of the few continuous processes for manufacturing of composite parts and enables the cost effective, high volume production of structural profiles, furthermore it's one of the fastest processes within the industry for manufacturing composite products [3,4].

Pultrusion is a continuous manufacturing system of composite profiles with a constant cross section. In this process the reinforcing fibers are immersed on liquid resin in resin bath or an injection box before the fibers and resin are heated in a die (where the curing process takes place). In pultrusion die region, after the temperature reaches the gel point, an exothermic reaction begins and the cure reaction is initiated. In (Fig. 2) and (Fig.3) is show a schematic of the pultrusion process [5,6,7,8].

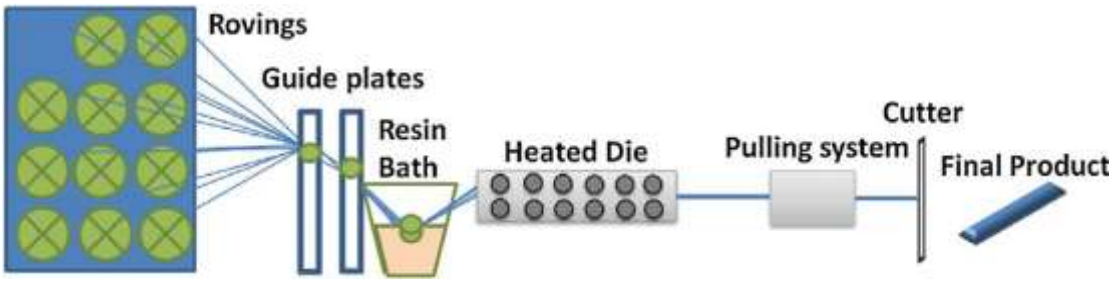

Fig. 2. A schematic of pultrusion process.

Fig. 3. A schematic of heating sections of the die pultrusion.

1.3. Purpose of Thesis

This work aims to optimize the pultrusion process in order to improve the degree of cure by optimizing die temperature. It also aims to present a study on kinetic parameter estimation of an epoxy resin using an empirical and phenomenological models and apply them in a simulation (ANSYS CFX) of pultrusion process.

The thesis will be show the characterization of the cure reaction of an epoxy resin typically employed in pultrusion manufacturing processes. It was computed the reaction kinetic using both an empirical and a phenomenological approach. The achieved kinetics were implemented in a thermochemical model of a pultrusion process developed within the software, ANSYS-17.2 suite. The values of temperature and degree of cure predicted using the two different kinetics are discussed and compared.

The objective function studied aims to minimize the heater temperatures in order to find a uniform degree of cure for all control volume. Two different approaches were used. One of the methodological approaches used in this thesis wasan exact quadratic programming based algorithm and it was also used one is a Particle Swarm Optimization meta-heuristic algorithm. The pultrusion process was modeled based on a total number of 16 heaters embedded in the die block, instead of external planar heaters. A quadratic programming algorithm and a heuristic particle swarm was used to optimize the manufacturing process.

Over the past few years, some works have been done on simulation studies for pultrusion analysis have been published. However, no work has been done on

studies focusing on the Phenomenological model along with the study of the mathematical model of the pultrusion process around the mold region in order to improve the degree of cure in this process. Thus the main focus of this thesis will be on a study of a Pultrusion of thermoset based profiles-state of the art regarding materials, process set-ups, process modeling, and process simulation model of Improving Degree of Cure in Pultrusion Process by Optimizing Die-Temperature. The (Fig. 4) presents the individual steps required to reach this goal.

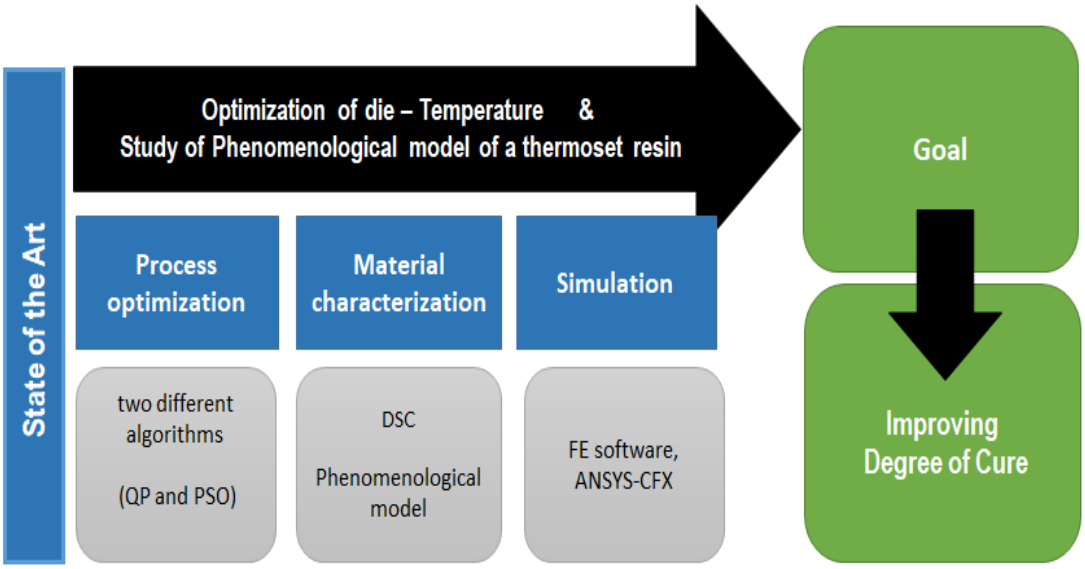

Fig.4. Flow chart of the addressed topics in order to reach the goal.

2 State of the Art

2.1 Brief Introduction to Polymeric Composite Pultrusion

As an overview, a composite is any multiphase material that significantly demonstrates the properties of both its constituent phases, such as stiffness and toughness, in order to obtain similar or improved properties, compared to the properties of each component individually [9]. A composite material is formed by a continuous phase called matrix and a dispersed or discontinuous phase consisting of fibers or reinforcements. When this continuous phase is consisting of a polymeric resin, the composite material is characterized as polymeric. The most widely used polymeric resins are polyesters and vinyl esters, matrices usually reinforced by glass fibers. Special additives may also be incorporated, such as UV protectors, antidust agents, colorants, etc. During the manufacture of a composite part, there is a resin cure reaction, polymerization reaction, on the reinforcement used. This process couples the two phases providing the resulting material with special final properties as well as changes substantial physical factors [10].

Many technologies used with combinations of properties that cannot be met by alloys, polymeric materials and usual ceramics. Among the advantages that polymer composite materials present are: flexible structure, low specific mass, low cost of high performance in harsh conditions such as corrosive media and high mechanical strength in relation to their weight. Nevertheless, the use of this type of material has advantages such as low toughness and limited reuse or recycling [9].

The properties of a given composite also depend on the matrix and the reinforcement chosen, which can add disadvantages, as the highest cost of using carbon fibers. The application of polymeric compounds emerged in aeronautics, with a need for to reduce weight while preserving the robustness of the structure. Currently, a large variety of composite materials can be found on replacement of metallic materials (fuselage, landing gear doors). The automotive, naval, aerospace and civil construction sectors are the most prominent in the use of this type of material. Based on their qualities and their Due to its wide applicability, the use of

polymeric compounds is increasingly worldwide, representing a large part of technological origin today [10,11].

There are different processes used to make composites: filament winding, RTM (Resin Transfer Molding), RIM (Resin Injection Molding), pultrusion, autoclave, among others. Among these, the pultrusion process is based on the production of parts with uniform cross section. Such a section can have different geometries according to the mold used, which can be either regular (rectangular or cylindrical) or irregular.

Pultrusion is a process in which fibers are continuously impregnated with a polymeric matrix and consolidated into a composite solid. To the solid part to form, the metal mold must be heated to provide a heat flux that activates the resin cure reaction. This heating is carried out by means of electrical resistors coupled to the mold metal, both on the surface and inside. Despite the limitation of the process, producing only components with constant cross section, it has low cost, simple machinery and a high level of automation [10,11,12].

In the 1950s, W. B. Goldsworthy, one of the pioneers in the plastics and composites industry, built the first idealized pultrusion equipment and filed a patent, initially for the manufacture of small diameter reinforced plastics intended for the manufacture of fishing rods. Pultrusion quickly gained notoriety for being a technique capable of produce sturdy parts with a constant cross section and because of their commercial advantages such as high production rates and reduced cost compared to other existing processes, such as the BMC (bulk molding compound) process. These advantages enabled the development of this industry, primarily in the US and, subsequently in Europe. In the 1970s, the first direct applications of engineering area, in the construction of household items such as shovels and ladders. In the years 80, the first applications in the construction industry began to emerge, the first large profiles such as bridges and walkways. Subsequently, materials pultruded products began to be applied in several other industries, such as automotive, making the fields of its use ever wider [3,13].

Due to the nature of the pultrusion process, reinforcement should be continuous, whether in the form of rovings, blankets or veils. The fibers are stored

in a shelf simple construction, because they should not normally support anything but of fiber weight. These shelves are often movable, with wheels at their bases for move around. Such mobility allows better adaptation to different needs depending on the desired profile, the number of fiber strands the food varies, and all or just a few rolls may be in use [13].

2.1.1. Material supply

Pultrusion, come from the terms pull and extrusion where the process is characterized by the continuous traction of fibers that are impregnated with polymeric resin. Once impregnated, the fibers are directed to a metal mold whose cavity has the shape of the desired profile for the part [14]. The fiber-resin mixture consists of the raw material and may contain additives such as dyes and catalysts. Thus In the simplest configuration of the pultrusion process the impregnation of the reinforcement is performed by capillary forces in an open resin bath. The fibers are then guided downward and into the resin bath. In a variant of this open bath soak, the reinforcement is guided in and out of the bath horizontally through side openings in the resin tank.

The pultrusion line is manufactured for the production of continuous fiber based polymer composite profiles (3). The process can be divided into the following parts: (1) Spool box: is the place where the dry fibers are placed and positioned in the first part of a pultrusion line; (2) Injection box: the resin is injected into the die under pressure and is forced into the interstices of the fiber system; (3) Heated die: the curing dies are heated with electric heaters. The heating system is equipped with thermocouples distributed along the die; (4) Pull machine: a cut-off saw is needed to cut the pultruded profiles.

The spool box is the place where the dry fibers are placed and they are positioned at the first part of a pultrusion line. In this storage area the fibre tows are drawn in the correct sequence to match the design requirements of the structural shape Fig. 5. Since pultrusion is a long run continuous process, fibre tows are provided in the maximum size configuration possible. Continuous glass tows are provided in “center pull” packages of 20 kg in size. These center pull packages are stored on a bookshelf style creel. These creels have from three shelves and are

capable of storing anywhere from 30 to 48 packages of this type of fibreglass. The casters are provided with a foot locking device to enable them to be locked in place when this is required. The fibers are pulled vertically from the box through holes in the shelves (see Fig.5 and Fig.6).

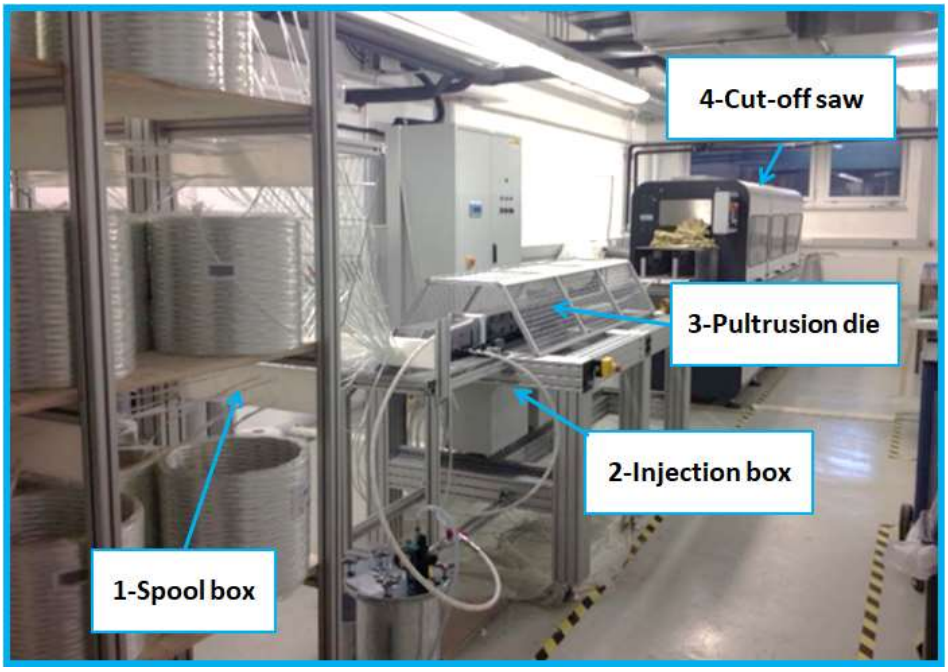

Fig. 5. Pultrusion line (Source: LVV, Montanuniversität Leoben).

Fig. 6. Spool box equipped with glass fibre tow spools.

The tow is collected above the creel and turned 90° by means of a HDPE type guider and then moved forward to the material accumulating section just prior to the injection box and forming die. The pulling of fibre from the center of the package will automatically insert a twist in the fibre as it is led into the pultrusion machine. As the fibre tows travel forward towards the injection box it is important to control the alignment of the fibre tows which are going into the configuration. This will prevent damage of the fiber and will also provide the right direction fibers relationship that will be placed in the correct zone of the pultruded composite material [15]. Generally, an open dip-type resin bath (Fig. 7) is used to impregnate the fibre where the fibre are passed through a resin bath. Environmental problems may be presented when using the open Pultrusion process due to emission of environmentally detrimental vapors, example the styrene in case of unsaturated polyester resin systems. To avoid this kind of problem the resin-injection system was created. However, both pultrusion processes are still used both the open pultrusion process and the resin-injection system [16].

Fig. 7. An open dip-type resin bath.

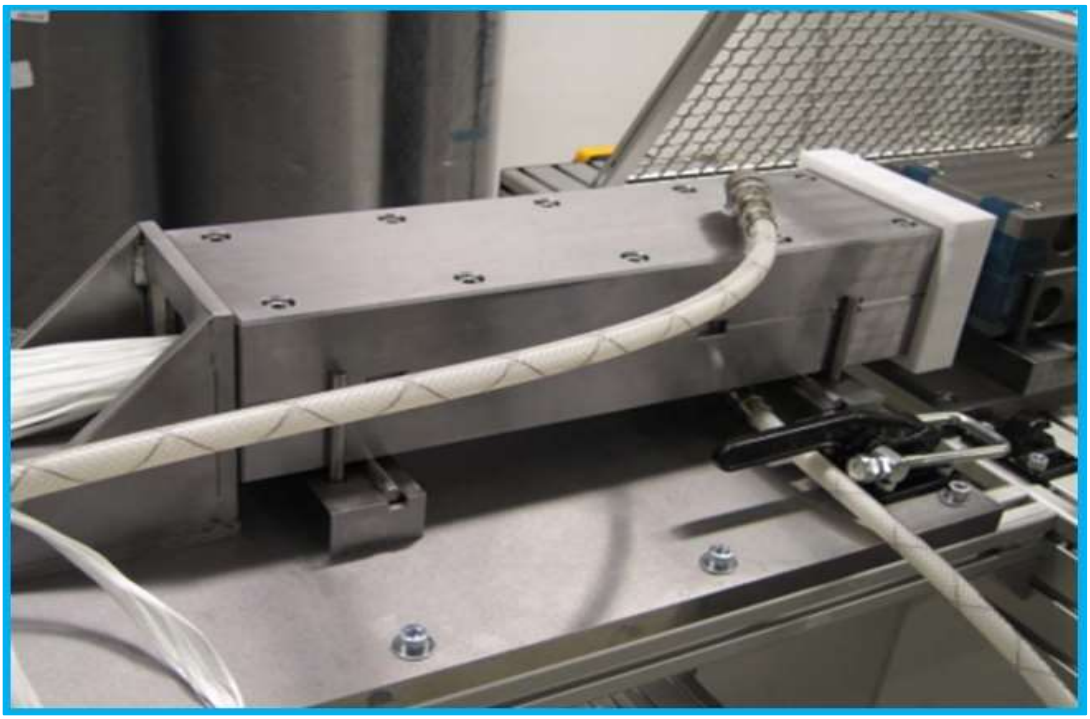

Fig. 8. Injection box with two injection points (LVV, Montanuniversität Leoben).

In Injection box (Fig. 8) the resin is directly injected in a forming die or in a initial segment of the pultrusion die. The resin is injected into the die under pressure and is forced into the interstices of the fibre system. The principal advantage of this system is that it limits the release of volatile resin components and reaction products.

An additional advantage of this process is the rapid resin change without removal and cleaning of all of the components.

2.1.2. Profile geometries - Pultrusion die

In the pultrusion process, the fibers are impregnated on resin (liquid) in a resin bath open or an injection box, then resin-wet fibers enter a heated mold by (external planar heaters or internal heaters) in which the curing process takes place. In this process, the heat flux provided by the mold (Fig.9) must be satisfactory to promote the cure of thermoset resin [5,6,7,8].

Fig. 9. Pultrusion die (LVV, Montanuniversität Leoben).

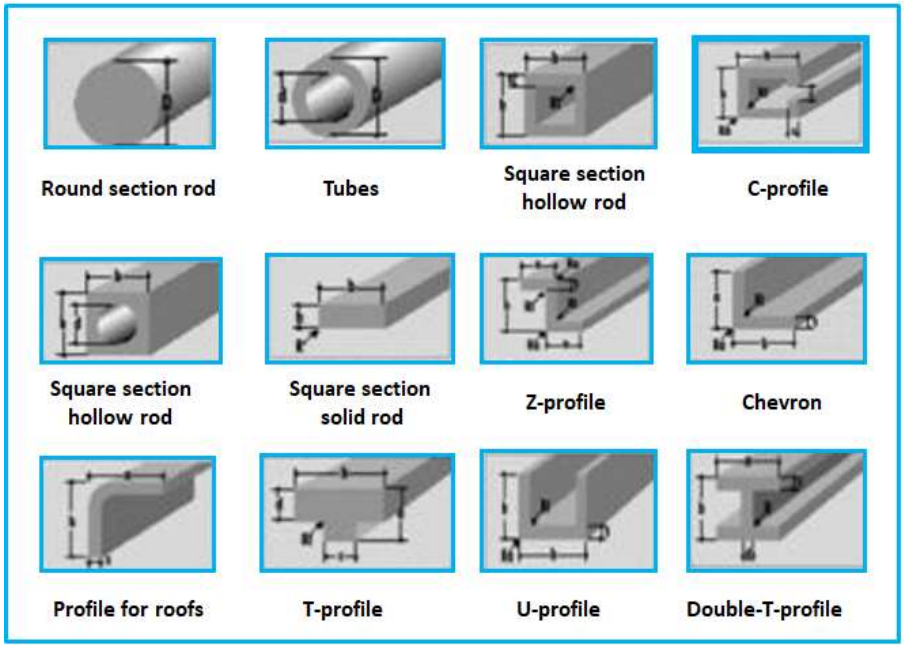

Fig. 10. Standard profile geometries. [16] (Source: EPTA- European Pultrusion Technology Association).

There are only a few methods for applying the matrix material to the process when using reactive thermoplastic matrix material.

During the pultrusion process the liquid resin can be injected directly into the die (injection box). This mode is known as Reactive injection Pultrusion (RIP). There will be impregnation in the resin, then the solidification and finally obtaining the composite material (forming of the profile). This will happen in the die before the resin thermoset (matrix) is transformed into the solid state. The (Fig.10) are show some profile geometries. [17].

2.1.3. Pulling force and Cutting machine

For the extraction of pultruded composite there are the most commonly used puller/clamp systems, but there is also the hydraulic reciprocating puller method consisting of two identical units which operate to grip and pull the profile. A system used in the pultrusion process is the Caterpillar-tractor method. This is a continuous belt-type system where the grips clamp to the part and the puller drag the part through the die [17].

Caterpillar type pulling machines are preferred and still widely used in the industry. The Caterpillar machine has many clamping pads (72), this high number of pads allows rush between the clamping pad. The pulling machine of our pultrusion line (Fig. 11) has an electric motor of 24kN and the grippers are made from aluminum that could work up to 100 degrees Celsius. The clamping mechanism is based on pneumatic cylinders that work up to 6 bar of pressure.

In order to cut the pultruded profiles a cut-off saw is used. The cut-off station of our pultrusion line (Fig. 12) has a cutting saw with diamond disc that could cut all the profiles produced by our pultrusion line. The cutting saw follows the pultruded part and cuts the composite profile at the desired length given by the user. It is mounted on a platform which moves down the pultrusion exit table at the same speed as the pultruded product.

Fig. 11. Pulling machine equipped with a cut-off station (Source: LVV, Montanuniversität Leoben).

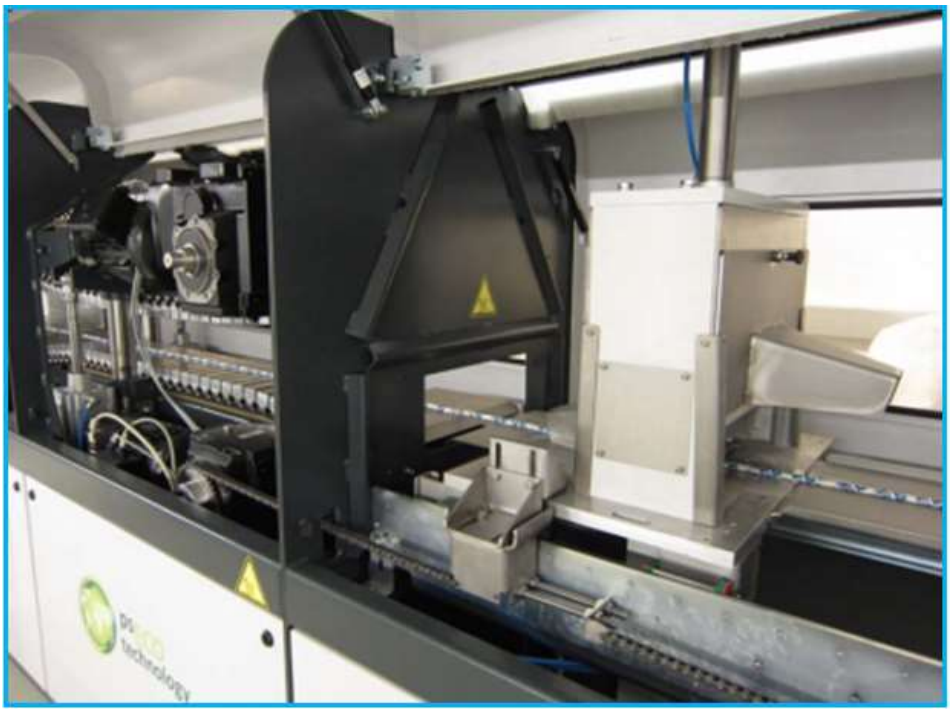

Fig. 12. Pulling machine equipped with a cut-off station (Source: LVV, Montanuniversität Leoben).

2.2. Commercial products and apllications

Pultrusion is one of the few continuous processes for manufacturing of composite parts and enables the cost effective, high volume production of structural profiles, furthermore it's one of the fastest processes within the industry for manufacturing composite products [16].

Composite materials are also used for wind turbine blades. An example of an innovative turbine is DeepWind (Fig.13), a vertical axis wind turbine that are based on onshore technology [16,18].

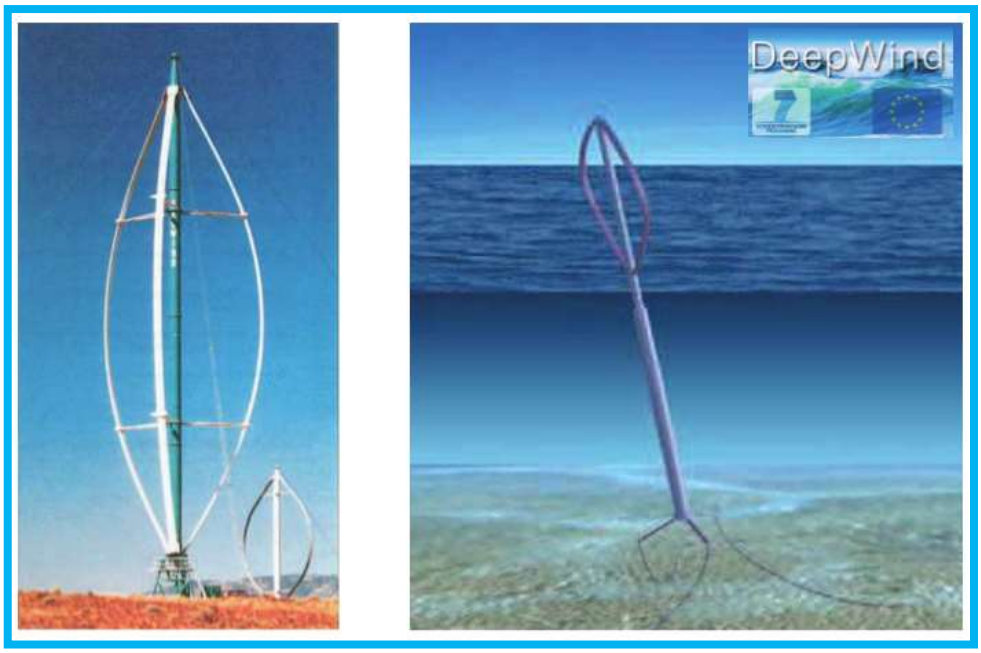

Fig. 13. Onshore Darrieus design in the FloWind (Figure Source [18]).

A current and innovative development for Pultrusion is the Radius Pultrusion (Fig. 14), which allows the production of arbitrarily curved profiles in the economic pultrusion process [16, 19].

Fig. 14. Radius pultrusion process (Figure Source [19])

2.3. A brief study of thermoset resin

The polyester resin is one of the most used in pultrusion process, followed by epoxy resin, due to its mechanical properties and heat resistance, there are also other resins used in this process such as vinyl ester resin, phenolic resin, thermoplastic resin. American Shell Company has developed two kinds of epoxy curing agent system, EPON 9102/CA 9150 and EPON 9302/9350 are CA curing agent, bisphenol A epoxy resin [20,21].

Epoxy resins were introduced commercially in the USA in the late 1940s. They have gained wide acceptance in the surface coatings industry due to their exceptional combination of properties such as toughness, adhesion, chemical resistance and superior electrical properties. Epoxy resins are characterized as compounds or mixtures of compounds which contain one or more epoxide or oxirane groups as shown in formula (Fig.15) [22].

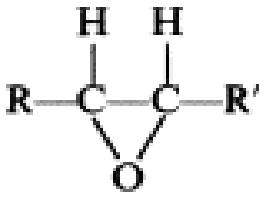

Fig. 15. Radius pultrusion process (Figure Source [22])

There are three major types of epoxy resins: cycloaliphatic epoxy resins (R and R ′ part of a six-membered ring), epoxidized oils (R and R ′ are fragments of an unsaturated fatty acid, such as oleic acid in soybean oil) and glycidated resins (R is hydrogen and R ′ can be polyhydroxyphenol or a polybasic acid). Epoxy resins derived from bisphenol A is the most commercially used in the pultrusion process. The most important constituent in epoxy resins is Bisphenol A and it is production by the condensation of acetone with phenol. The latter two compounds can be prepared in the Hock process by the oxidation of cumene. Phenolic products are shown in (Fig. 16) [22]. The epoxy resin is composed of some formulations, such as: epoxy resin (base), the curing agents, and for the contribution of the mechanical properties of the composite product it is necessary the addition of modifiers [22].

The interest in using bisphenol A resin in the pultrusion process is due to its performance characteristics of these resins are imparted by the bisphenol A moiety (toughness, rigidity and high temperature performance), the ether linkages (chemical resistance) and the hydroxyl and epoxy groups (adhesive properties and formulation latitude, or reactivity with a wide variety of chemical curing agents).

Glycidation is the most commonly used reaction to introduce epoxy functionality and resins and prepolymers. The most used epoxy resins are based on diglycidyl ether of bisphenol A, derived from the reaction between bisphenol A and epichlorohydrin. These resins are di-functional as they theoretically contain two epoxy groups per molecule. The Fig. 17 shows the synthesis of an epoxy resin based on bisphenol A, from the formation of its monomers to resin ready for the crosslinking process.

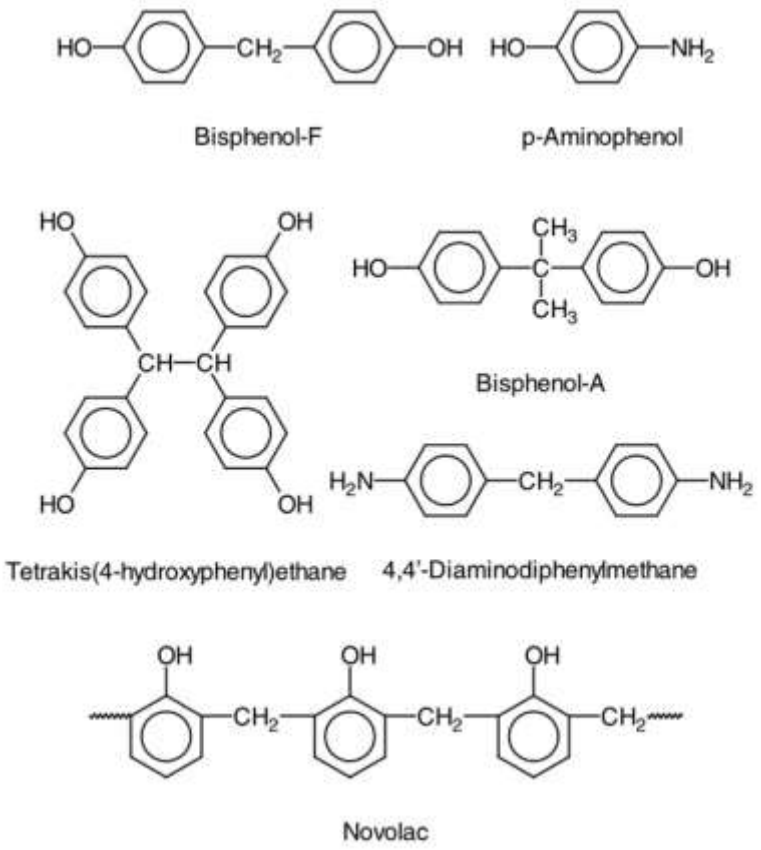

Fig.16. Compounds for epoxide resins [23].

Initially, the formation reaction of glycidyl ether chloride is made from ethylene and the reaction of bisphenol A is made from benzene. The final reaction of glycidyl ether chloride and bisphenol A results in the diglycidyl ether of bisphenol A (DGEBA), which is the epoxy resin itself. After this step, the prepolymer is ready to react with suitable curing agents and assume its final molecular form as a crosslinked resin.

The epoxy resins used in pultrusion processes are resins based on simple or modified bisphenol A. The degree of cure offered by systems like these tends to decrease with increasing molecular weight. Thus, with the increase in molecular weight, the resin becomes more solid, so that it is more difficult to mix the resin and

the curing reagent. Thus, small amounts of epoxy groups by weight of resin react, resulting in moderate resins, with considerable thermal and chemical resistance.

Resins with high molecular weights or high levels of epoxy groups by weight of resin have flexibility and toughness and other beneficial characteristics in the mechanical properties of the pultruded material. However, for Pultrusion epoxy resin systems, resins with lower viscosities are more suitable for the process. Resins with lower viscosity offer better wettability of the reinforcements, ensuring a good impregnation [24].

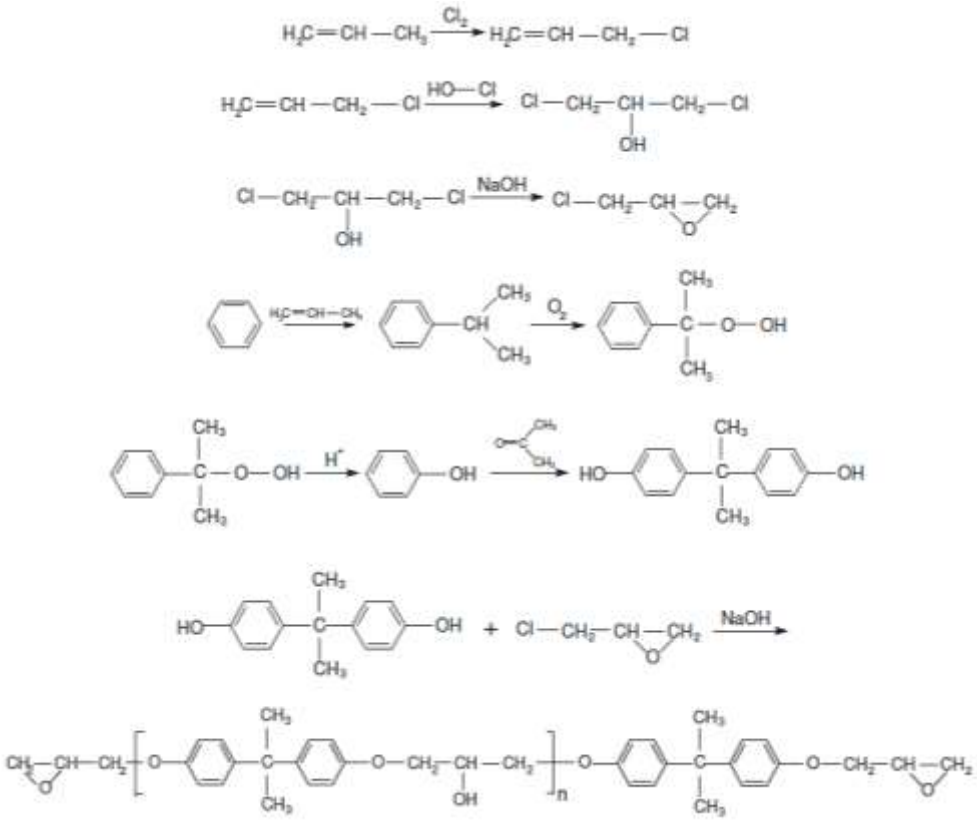

Fig.17. Synthetic reaction and molecular structure of diglycidyl ether of Bisphenol A (DGEBA resin) [24].

2.4. A study for modelling the thermosetting resin.

The curing reaction of epoxy systems is not trivial process and can be defined as changing the physical and chemical properties of a reagent / resin formulation [25,26]. In experimental pultrusion process, there are difficulties that can be resolved by a study that requires knowledge of the transport phenomena involved, which implies use of mathematical models to predict the physicochemical behavior of the process. For such studies, the mold is usually considered to be the main part of the process, as it is the area where most of the cure reaction and heat transfer takes place. Heat transfer is defined by the thermal energy in transit due to temperature differences. The transfer of energy as heat occurs at the molecular level as a result of a temperature difference [26].

Studies on the evaluation of kinetic parameters from data obtained through thermal analysis were published in the last years [27, 28, 29, 30, 31, 32, 33]. Pagano et al. In [29] the authors present a new approach for parameter estimation kinetic cure model of thermosetting. A differential-algebraic approach is used for resin estimation.

A significant contribution regarding this subject is the work of Sbirrazzuoli and Vyazovkin [34], who compared two computational models that addressed kinetic evaluations: An approximation of reaction models for simple heating rate and an advanced isoconversional method that eliminates the approximation model in a single step and replaces it using multiple heating rates [35, 36]. Sbirrazzuoli and Vyazovkin [34] studied the cure of the epoxy resin by means of the isoconventional model-free analysis using isothermal and nonisothermal DSC (Differential Scanning Calorimetry) and proved the dependence between the activation energy and the extension of the curing reaction. Recent works on isothermal and non-isothermic curing kinetics modeling of an epoxy resin system are presented by Javdanitehran et al. [37]. In [38] a work is presented on a new equation to describe the effect of diffusional limitations on the cure kinetics of epoxy-amine resins. According to the results, a satisfactory agreement of the model equation with the experimental data could be attained. In [39] authors present an important contribution of the dissolution of molecular species to the activation energy on isoconversion analysis of the data,

showing low temperature and high degrees of curing. An estimation of the kinetics was performed using an Arrhenius law and nth order autocatalytic model.

As said, numerous authors have proposed different models for the prediction of the kinetic parameter of curing reaction. Most of them are empirical models that reproduce only the evaluation of the degree of cure throughout the reaction, without considering explicitly the polymerization reaction mechanism. Therefore, these models generally involve few kinetic parameters, which can be estimated from Differential Scanning Calorimetry (DSC) data [29]. However, empirical models are limited in terms of providing a full comprehension of the system due to the lack of information regarding the full kinetic of the functional groups [29].

Some researchers have proposed kinetic mechanisms to describe the curing behavior of epoxy-anhydride system [40, 41, 42, 43]. In Antoon et al. (1981), [44] the mechanism for amine-catalyzed epoxidelanhydride copolymerization was developed. The authors suggested a kinetic model, which describes the kinetic rate of the principal components involved in the curing process. Some experimental results were obtained by the use of NMR spectrometry. Amirova et al. (2016) [43] proposed the kinetic mechanism of an epoxyanhydride curing with phosphonium salts as accelerators. The results showed that the phosphonium salt accelerates the curing via electrophilic attack at the phthalic anhydride. A deeper discussion on kinetic mechanism to describe the cure of epoxy resins can be checked in [45,46,47,30]. As can be seen, although there are already some studies that discuss kinetic mechanisms for curing epoxy resin, kinetic models that make it possible to simulate the system are still scarce. In addition, the incorporation of more complete models for the simulation of the pultrusion process has not yet been evaluated.

2.5. Numerical simulation

Some work on the pultrusion process has been published. In [45], the authors attacked the problem by optimizing pulling speed and the boundary conditions imposed on the die wall. In this study [46] researchers worked on the optimization to fi nd the optimal cure temperature profile under uncertainty conditions, in order to achieve the objective of improving the curing uniformity of the composite material it was used a finite-element (FE) package to evaluate the kinetic heat-transfer and

cure of the process [5,6,7,8]. The authors used the finite difference method to solve the model and a combination of simplex and genetic algorithm methods to find the optimum cure cycle. In [47] researchers show a study on the optimization of the pultrusion system, minimizing the energy consumption during the cure reaction in an injection pultrusion process. In [48] the authors made use of finite difference method to simulate pultrusion process, and subsequently proposed a hybrid optimization algorithm approach combining the simplex method and genetic algorithm, to improve the dimensional accuracy of fabricated parts.

In [49] the authors proposed internal heaters to be coupled inside the pultrusion die. The goal was to increase the number of available arrangements to find the optimal arrangement minimizing energy consumption. The study on the configuration with internal heaters allows more uniform curing while minimizing the energy consumption is discussed [50].

In [51] a mixed integer genetic algorithm was used to increase the productivity of the pultrusion process. The number of heaters was minimized while satisfying the maximum temperature and the pulling speed constraints [52].

2.6. Computational fluid dynamics (CFD)

Computational fluid dynamics (CFD) can be briefly described as the numerical simulation of engineering problems that involve fluid flows. These problems may or may not have other physicochemical phenomena beyond the fluid dynamics involved, such as reactions chemicals and heat and mass transfers. CFD packages are designed to be capable of predicting velocity, pressure and concentration fields, properties and temperature profiles by domain discretization models studied based on momentum, mass and energy conservation equations.

There are a number of CFD business codes, such as those distributed by ANSYS, such as CFX, Fluent and Abaqus/CFD.There is also open source such as OpenFOAM. The computational packages are also highly recognized for their efficiency and applicability, being used in various industrial and study areas, such as Chemical industry in general, with an emphasis on the petrochemical sector, including food industry; Automotive and aerospace sectors; Architecture and

construction etc. Thus to solve a CFD problem, the following steps must be followed sequentially.

- Definition and design of geometry;
- Geometry discretization, generating domains (mesh generation);
- Definition of mesh regions, boundary conditions, phenomena, equations and parameters (preprocessing);
- Convergence of simulation (solver);
- Analysis of the results obtained (post processing).

In the preprocessing step for the computational field simulation is the discretization of the domain of interest and is called mesh generation. The process of mesh generation can be broadly classified into two categories based on the topology of the elements that fill the domain. The meshes are nothing more than the domain to be studied discretized; that is, the domain is made up of small finite elements. When the mesh has very small elements, it is said to be highly refined. The refinement of the mesh is fundamental, since the smaller the elements, the more accurate the results from the simulation. There are two types of meshes, known as structured and unstructured meshes. A structured mesh is defined as a set of hexahedral elements with an contained connectivity of the points in the mesh. An unstructured mesh is as a set of elements, commonly tetrahedrons, with an established connectivity.

Domain discretization can be in different ways. The main discretization techniques are: finite elements, finite differences and finite volumes.

The finite element method (FEM) is mainly used in the area of structural analysis in order to determine the stress and strain state of a solid. One of the most important tasks in developing a product is determining it is structural behavior and ensure that there will be no failures under normal operating conditions as well as in critical situations. This method is one of the main tools to determine such behavior [53].

The finite difference method (MDF) has as its fundamental principle to approximate, by algebraic expressions, each term of the mathematical model,

constituted by partial differential equations in each mesh node. This is done based on the Taylor series approximation of the derived function [54].

Similar to the finite difference method, the finite volume method (MVF) evaluates partial differential equations in the form of algebraic equations. In this technique, volume integrals in a partial differential equation that contain divergent terms are converted to surface integrals (Divergence Theorem). Thus, these terms are evaluated as property flows on the surfaces of each volume. The flow that exits an element must be identical to the flow that enters the element.

2.7. Finite volume numerical method

The finite volume method was introduced by Patankar in 1980.Patankar developed the method for use in solving heat transfer and fluid flow problems.The finite volume method is dominant throughout the field of CFD for solving the kinds of partial differential equations encountered in this area [55,56].

The solution domain is discretized by an unstructured mesh composed of a finite number of contiguous control volumes (CVs) or cells. Each control volume is bounded by a number of cell faces which compose the CV-surface and the computational points are placed at the center of each control volume [56,57].

Control volume

In thermodynamics, a control volume can be defined as a fixed region in space where one studies the masses and energies crossing the boundaries of the region. The surface of the control volume is referred to as a control surface and is a closed surface. The surface is defined with relative to a coordinate system that may be fixed, moving or rotating. As all variables are stored in the nodes, for the problem to be solved it is necessary to create an equation for each node, that is, a volume control for each point. It is therefore consistent that the volume of control is created around these nodes (points). The Fig. 18 shows this volume that is formed with four quadrants, each belonging to one of the four elements to which this node is common. For simplicity, the lines of s = 0 and t = 0 were chosen as faces of the control volume [57].

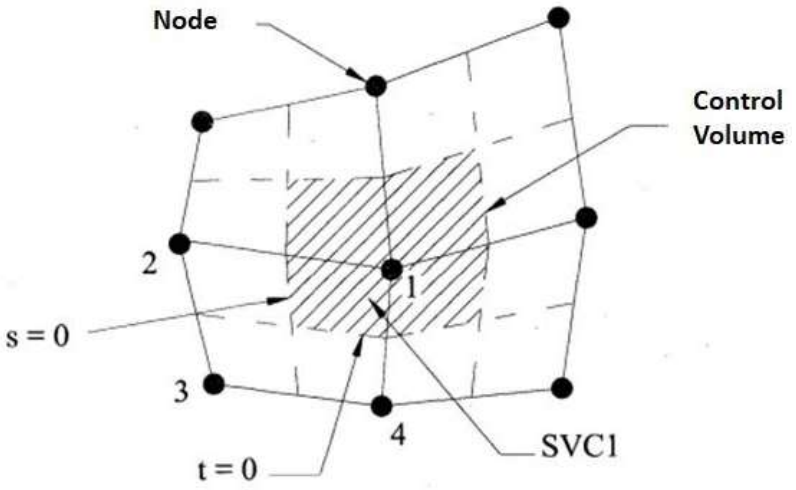

Fig.18. Control volume [57].

2.8. Pultrusion Die – Mathematical model.

In the pultrusion process the mathematical model on the die region is conducted by mass and energy balances, (see equation 1) [58].

$$\rho_c Cp_c\left(\frac{\partial T}{\partial t}+w\frac{\partial T}{\partial z}\right)=\nabla\left(\bar{k}_c\nabla T\right)+\frac{\partial H}{\partial t} \tag{1}$$

Where ρ_c is composite density; C_{Pc}, the composite specific heat; k_c the composite conductivity: w, the pull-speed; z is the pull direction, t; the time and ∇ the gradient operator and subscript c denotes composites. The $\frac{\partial H}{\partial t}$ describe the rate of heat generation which corresponds to cure reaction. It is reasonable to assume that the cure time is higher than the resin flow time [5,6,7,8]. The mass balance, in terms of concentration, may be expressed as:

$$\frac{d\alpha}{dt}=r_a \tag{2}$$

where α is the degree of cure and r_a denotes the reaction rate.

For the kinetic study of the pultrusion process it is necessary to work with the kinetic equation, thus two kinetic models were used here: (i) an nth order empirical kinetic model and (ii) a phenomenological kinetic model.

2.9. FE-Nodal control volume- Optimization

In Pultrusion process the region enclosed by the die is considered as the main part of the process. The mathematical model of the Pultrusion process around the die region is governed by the mass and energy balances (see the session (2.7). The term $\frac{\partial H}{\partial t}$ defines the rate of internal heat generation due to cure reaction and is expressed as:

$$\begin{aligned}\frac{\partial H}{\partial t} &= \rho_r V_r H_t \left[\frac{\partial \alpha}{\partial t} + w\frac{\partial \alpha}{\partial z}\right] \\ &= \rho_r V_r H_t \left[B_0 \exp\left(\frac{-\Delta E}{R(T+273.15)}\right)(1-\alpha)^n + w\frac{\partial \alpha}{\partial z}\right]\end{aligned} \tag{18}$$

Thus, α is degree of cure, H_t describe the total heat of reaction per unit mass of resin, v represents the volume fraction, the activation energy is ΔE, R the universal gas constant, the pre-exponential constant (B_0), the order of cure reaction (n), and subscript r the resin. $\frac{\partial \alpha}{\partial t}$ portrays the rate of cure reaction. It is common to use Arrhenius type of reaction models for describing curing of resins, see [48].

The FE analysis is conducted over a small time-increment Δt. The time increment is chosen in such an approach that, Δt the preform moves at given w by interval Δz, which is the same to the dimension of one finite element in direction *(z*). For each control volume, T, and (α) assumed constant over Δt.

The convective effects on T and (α) resulting from the movement are included by calculating the terms in Equation (1) and in Equation (18), respectively, for each control volume, and superimposing them into the results for the previous

time step, see [46,59]. The procedure is iterated for the next Δt. using as a new boundary condition. The simulation is terminated, once the composite temperatures take on steady state. The degree of cure was assumed to be zero $(\alpha = 0)$ see in Fig. 19.

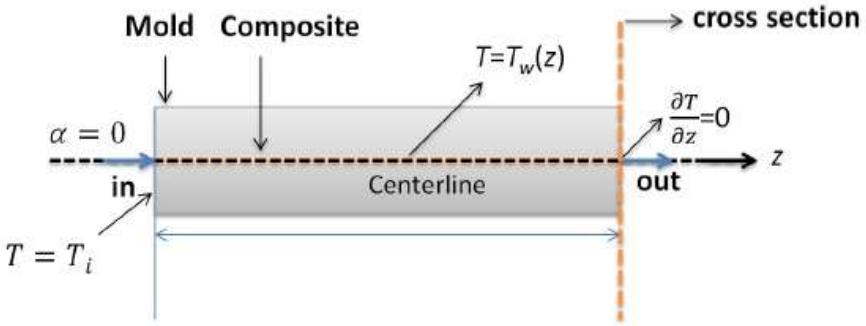

Fig.19. Schematic view of the process boundary conditions.

2.10. Particle Swarm Algorithm (PSO)

A particle swarm algorithm is a population-based stochastic optimization meta-heuristic. It was developed by Eberhart and Kennedyin (1995) [60]. The (PSO) algorithm is initialized with a population of random candidate solutions, conceptualized as particles (or individuals). The particles is attach an aleatory velocity and is iteratively propel through the search space. Each particle is attracted towards the location of the best fitness (according to the optimization criterion) achieved so far by the particle itself and by the location of the best fitness achieved so far across the whole population (see [61]). The following equations are used to describe the particle swarm displacements:

$$v_{i,d}^{k\,\mathrm{int}+1} = v_{i,d}^{k\,\mathrm{int}} + c_1 r_1 \left(p_{i,d}^{k\,\mathrm{int}} - x_{i,d}^{k\,\mathrm{int}}\right) + c_2 r_2 \left(p_{global,d}^{k\,\mathrm{int}} - x_{i,d}^{k\,\mathrm{int}}\right) \tag{19}$$

$$x_{i,d}^{k\,\mathrm{int}+1} = x_{i,d}^{k\,\mathrm{int}} + v_{i,d}^{k\,\mathrm{int}+1} \tag{20}$$

Thus, $k\text{int}$ is interaction, the speed is represented by v ; the position in search space is described by x; the particle are (i and d) and search direction; c_1 and c_2 are two positive constants. The best point (Pi) by the particle (i and P_{global}) is the best value found by the whole swarm [5,6,7,8,60].

In order to compute the temperatures (die-heating) the function provided in [61] is used associating the mold heating temperatures and the traction speed with the degree of cure of the pultruded material.[1,2,3,4,49,62].

2.11. Algorithm (QP) - quadratic programming algorithm.

The uniformity of the algorithm (QP), as defined in [63], is presented by function (21):

$$f(x) = \frac{1}{2} x^T Hx + b^T x + c \tag{21}$$

where, H is a symmetric and semi definite matrix; the vector is represented by (b) and (c) is a scalar. Thus, the optimization problem can be written as follows:

$$\min \{ f(x) : x \in S \} \tag{22}$$

Thus, the set of feasible solutions is described by (*S)*. In this case *(S)* will be the set of admissible die-temperatures and pull speeds.

The objective function that governs the optimization, in this case (die-temperature in pultrusion) will be the function suggested in [64]. The, quadratic programming algorithm, is an exact algorithm, thus the solution found is approve to be an optimal solution. In Fig.20 it is possible to see a flowchart of quadratic programming algorithm, technique is presented [65, 66].

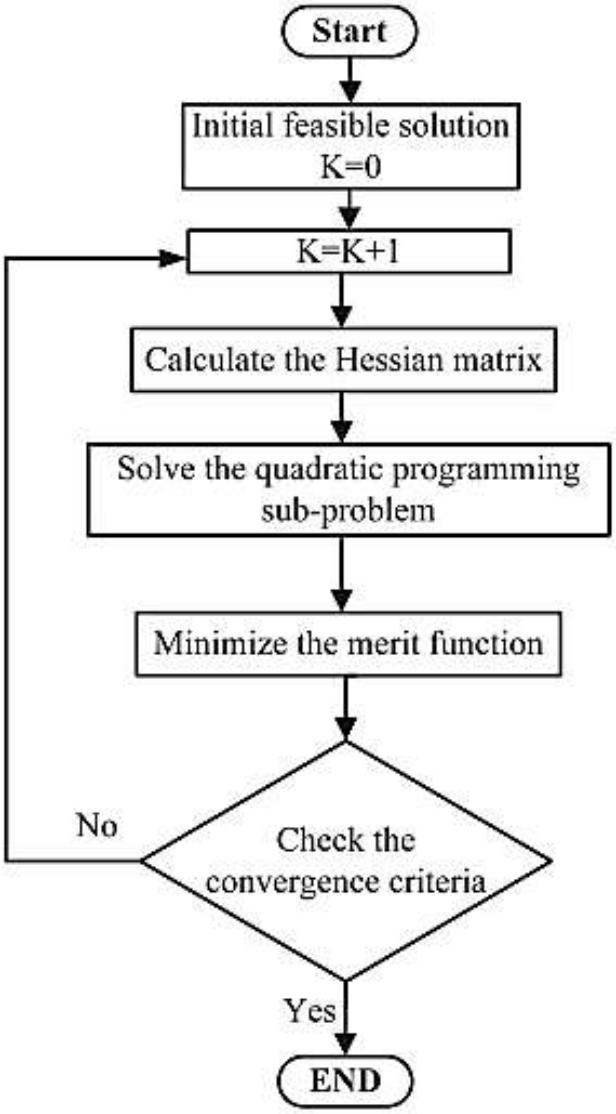

Fig.20. Flowchart of QP technique [66].

2.12. Empirical kinetic model

In this model, a simple Arrhenius expression to represent the cure of an epoxy resin is suggested according to Equation 3:

$$r_a = \left(Ae^{\left(-\frac{Ea}{RT}\right)} \right)(1-\alpha)^n \qquad (3)$$

where the frequency factor is (A), the reaction order is (n), the universal gas is (R) constant and the activation energy is (E_a.) Such model has been used recently by some authors: [5,26, 66].

2.13. Phenomenological kinetic model

The phenomenological model proposed here is based on the kinetic mechanism proposed by Antoon et al. (1981) [44]. The curing mechanism of an epoxy resin or the type of functional group of curing agent is an essential factor determining the structure of the cured resin. In the present model, an epoxy resin derived from an unmodified liquid diglycidyl ether of Bisphenol A (DGEBA resin) in a mixture with an Anhydride Curing Agent and an Accelerator like DMP-30 (2,4,6-tris(dimethylaminomethyl) phenol) was characterized. Based on these arguments, the suggested curing mechanism, used to represent the cure kinetic is represented in Fig. 21 [44].

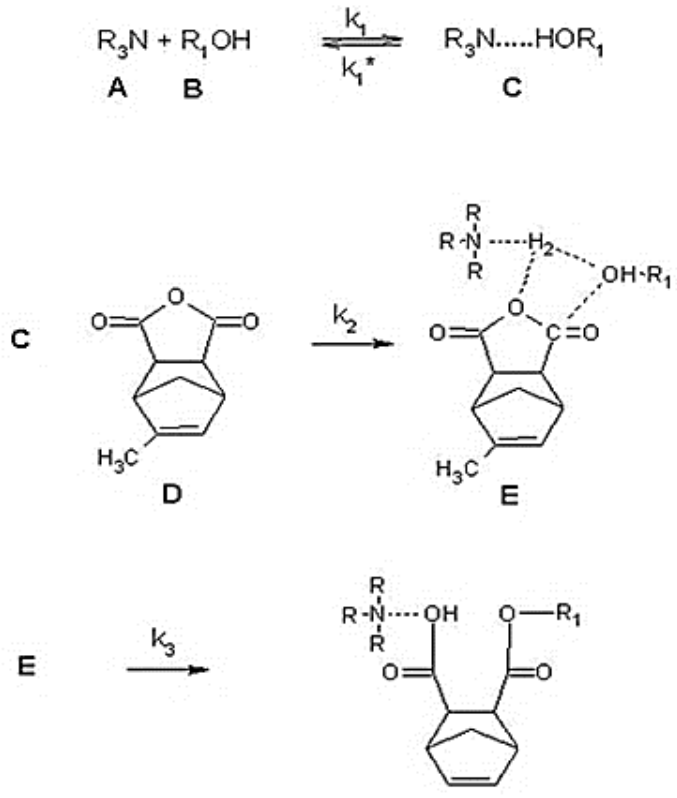

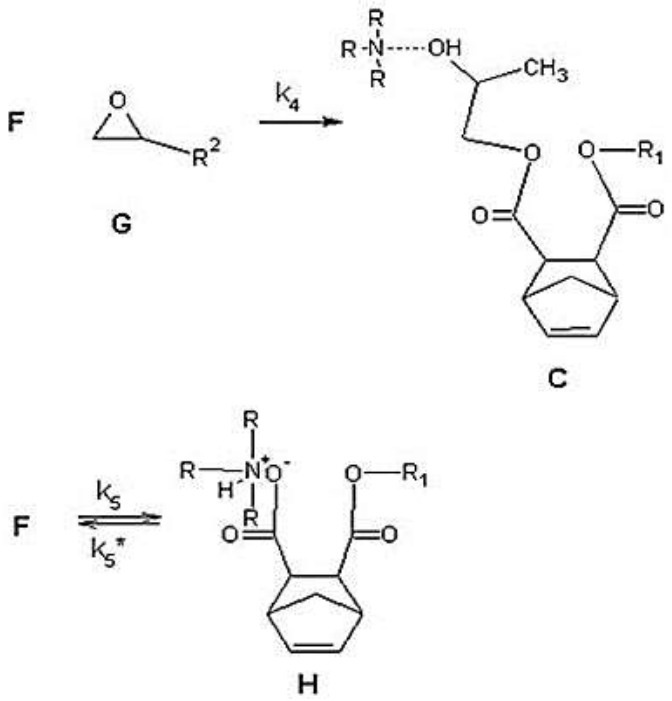

Fig.21. Proposed mechanism of cure reaction [44].

In which A represents the catalyst, B represents the epoxide molecules, D is the anhydride curing agent and G is the epoxyde group. The kinetic model can be written as:

$$\frac{dA}{dt} = -k_1[A][B] + k_1^*[C] \quad (4)$$

$$\frac{dB}{dt} = -k_1[A][B] + k_1^*[C] \quad (5)$$

$$\frac{dC}{dt} = -k_1[A][B] + k_1^*[C] - k_2[C][D] + k_4[F][G] \quad (6)$$

$$\frac{dD}{dt} = k_2[C][D] \quad (7)$$

$$\frac{dE}{dt} = -k_2[C][D] - k_3[E] \quad (8)$$

$$\frac{dF}{dt} = k_3[E] - k_4[F][G] - k_5[F] + k_5 * [H] \quad (9)$$

$$\frac{dG}{dt} = -k_4[F][G] \quad (10)$$

$$\frac{dH}{dt} = -k_5 * [H] + k_5[F] \quad (11)$$

Assuming that the concentration of active species remain constant [44] (stationary state is assumed), the Equations (6), (8), (9), (11) are represented by:

$$\frac{dC}{dt} = \frac{dE}{dt} = \frac{dF}{dt} = \frac{dH}{dt} = 0 \quad (12)$$

Resulting in:

$$\frac{dD}{dt} = \frac{dG}{dt} = -\frac{k_1 k_2}{k_1 *}[A][B][D] \quad (13)$$

According to this model, the rate of polymerization of epoxide groups is predicted by this equation and is proportional the concentrations of tertiary amine $[A]$, catalyst $[B]$, and anhydride $[D]$.

In order to obtain a new kinetic model, the kinetic model of the cure (previous) and the term diffusion [67] describing the diffusional effects were joined.

$$\frac{dD}{dt} = \frac{dG}{dt} = -f.\frac{k_1 k_2}{k_1 *}[A][B][D] \quad (14)$$

In which:

$$f = \frac{1}{1 + e^{(C \cdot (\alpha - \alpha c))}} \tag{15}$$

where α is the degree of cure, C is a constant and α_C is the critical fractional conversion. The degree of cure can be computed according to Equation (16):

$$\alpha = 1 - \frac{[G]}{[G_0]} \tag{16}$$

where $[G]$ is the concentration of epoxy and $[G_0]$ is the feed concentration of epoxy resin. The reason for including the diffusion parameter is justified by the limit on the reaction provoked by gelation/vitrification at high extents. According to Finkel, as the extent of cure progresses in a thermoset, the material first undergoes gelation followed by vitrification. Thus, it may impose a diffusion limit on the reaction.

The Arrhenius expression was used to incorporate the dependence of kinetic parameter with temperature:

$$k = A_0, ie^{(-Ea,i/RT)} \tag{17}$$

where A_0 is the pre-exponential factor, Ea is the activation energy, T is the temperature and R is the universal gas constant.

Effect of Diffusional Limitation

According to Corsetti et al. (2013) [67], as the reaction progresses, two different effects take part in the mechanism and change the dynamics of the system: autocatalysis and diffusion control. The autocatalysis occurs due to the generation of the hydroxide grous, which work as catalysts for the reaction, increasing the rate of reaction. However, as the extent of cure progresses in a thermoset, the curing

reaction is followed by vitrification, which imposes a diffusion limit on the reaction. Hence, modeling the cure kinetics of epoxy thermosets requires also a description of how diffusional limitations influence the curing reaction.

The term used to describe the diffusional effects is combined to previous kinetic models for the curing reaction of epoxy systems [68].

$$\beta = \frac{1}{1+e^{(C.(\alpha-\alpha c))}} \tag{18}$$

Where α is the degree of cure, *C* is a constant, α_C is a critical fractional conversion and *β* is the diffusional factor. In this regard, the degree of cure can be computed according to the Eq.19

$$\frac{dD}{dt} = \frac{dG}{dt} = \frac{k_1 k_2}{k_1{}^*}[A][B][D] \cdot \beta$$

3 Methodology – Numerical optimization (Pultrusion die).

3.1 Procedure – Optimization Steps

The heat flux provided by the heaters, in pultrusion process, must be sufficient to provide the curing of the thermosetting resin (matrix). Due to exothermic reaction, the temperature commonly reaches a maximum value inside the mold. Then decreases in the end stage of cure reaction [62].

The equation (23) presents the calculation the uniformity of cure. The measurement is due to calculating the root mean square deviation of the composite values degree of cure (in the mold outlet section) [9,62]..

$$f(\alpha) = \frac{1}{N-1}\sum_{i=1}^{N}\left(\alpha_i - \alpha^{\max}\right)^2 \tag{23}$$

Thus, $\alpha^{\max}$ is the degree of cure at each grid point (desired value to be found). The (*N*) is the number of nodes into the composite cross-section. The optimization problem can be formulated as show Equation (24):

$$\min \frac{1}{N-1}\sum_{i=1}^{N}\left(\alpha_i - \alpha_{desired}\right)^2 \tag{24}$$

$$T_{\min} \le T \le T_{\max,} \tag{25}$$

Where T is the vector

$$T = (T_1, T_2, ..., T_{M-1,} T_M) \tag{26}$$

belonging to R^M, M being the number of die heaters.

There are other constraints of this optimization problem, thus an equation (18) and equation (19) show the system of partial differential equations.

The optimization procedure summary implemented by [62] is recalled below:

i. Before starting heat transfer modeling it is necessary to set the initial temperature boundary conditions. Ascribe $T_{0,1}$ (initial temperature) for the *i-th* heater (mold),for $i = 1,...,m$. And, let $T^{k,i}$ be the temperature of *i-th* die heater at *k-th* iteration.

ii. It while keeping the temperature of the other heater fixed, the temperature of each heater is alternated. Thusly, due the modification in temperature of heater (*i)* , the change in degree of cure $\Delta\alpha$ of a control volume at the exit-cross-section of the composite, is displayed as:

$$(\Delta\alpha)_j^{k,i} = \left(\alpha_j^{k,i} - \alpha_j^{k-1,i}\right)/\left(\varepsilon\right)^{k-1,i}, k \geq 1 \tag{27}$$

Where (α_j^{k-1}) describe the degree of cure of control volume (j) at the precedents die heating conditions and ($\alpha_j^{k,i}$) describe the degree of cure of control volume (j) at the current optimization iteration, when the temperature of (*i-th*) heater is changed by a fixed small value (ε). Hence with this change on temperature of the *i-th* heater the degree of cure in a given volume at exit of the die due to any temperature change effects in the m heaters can be approximated [5,6,7,8].

$$(\Lambda)_j^k = \alpha_j^{k-1} + \sum_{i=1}^{m} \left(\Delta T\right)^{k,i} \left(\Delta\alpha\right)_j^{k,i} \tag{28}$$

Thus, $\left(\Delta\alpha\right)_j^{k,i}$ represents the change in α for control volume j per unit change in the *i-th* heater temperature at iteration k the optimization problem (8) is to be solved.

Three algotithms are used in this doctoral work to optimize the mold region of pultrusion process. The temperature conditions (bounds of decision variables) for the optimization were set at 177 °C ($T_{\min}$) and 227 °C ($T_{\max}$). The limit of the degree

of cure being 0.9 ($\alpha_{desired}$). A flowchart detailing the methodology is presented in (Fig. 22).

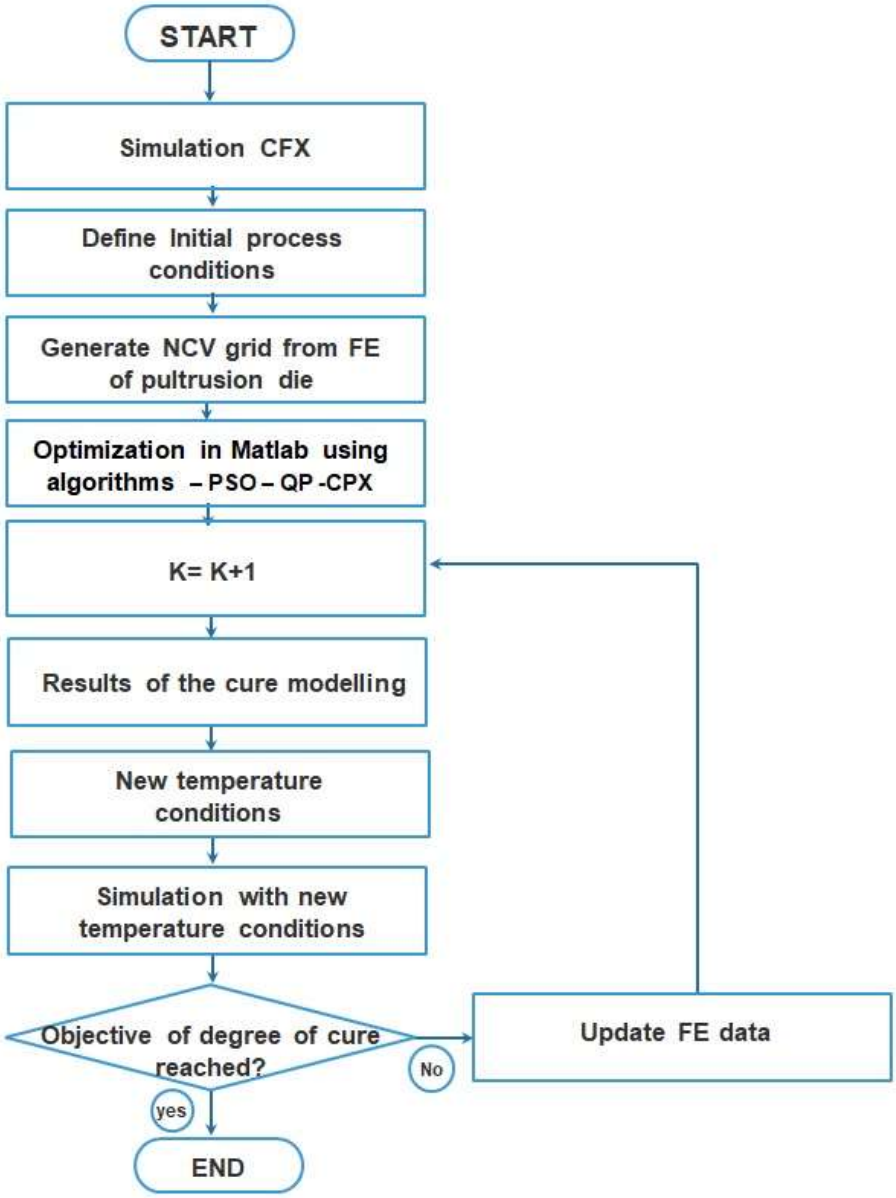

Fig.22. Flowchart of optimization

3.2 Simulation Steps

Geometries: Two different geometries are considered.

i. Geometry composite (A) – Pultrusion die.

For the Pultrusion system (C-section). A total of six heating pads, see (Fig. 23), each width, and height corresponds to 915 mm, 72 mm, respectively. The pultrusion and geometry system used to validate the model [23] is presented in (Fig.24) The planar heating abide of six steel heaters on convective boundary conditions and with dimensions length of 225 mm and 72 mm.

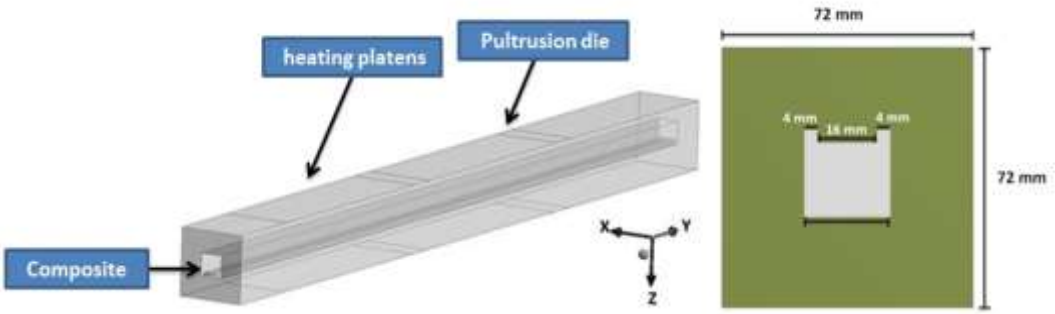

Fig.23. Dimensions of the cross section of the C- Shaped die.

ii. Geometry composite (B) – Pultrusion die.

The second pultrusion system to be simulated is presented in (Fig.24) and is part of the Pultrusion line of the Department of Polymer Engineering and Science at Montanuniversität Leoben. Thus the geometry consists of heating system consisting of sixteen steel cylindrical internal heaters with 10 mm diameter, and a, and height corresponding to 800 mm, 100 mm, respectively.

Fig.24. Pultrusion die (internal heater).

4 Case Studies – Simulation of pultrusion process.

4.1 Case study (Validation case)

Case study 1 and 2

In order to validate the simulation of the model studied by Joshi et al (2003) [59] a simulation was prepared for a C-Shaped die composite profile (see Fig. 23). The total of 6891 nodes and 27518 tetrahedral elements were used to create the FE model in Ansys-CFX. (see Fig. 25). In this work [59], researchers used epoxy resin EPON 9420/9470/537 and as reinforcement was used glassfiber. Resin and fiber properties are presented in Table 1. The kinetic parameters properties of the materials used in the simulation of the resin correspond to B0 = $1.914\times10^{5}(s^{-1})$, $\Delta E = 6.05 \times 10^{4}$(J/mol), R = 8.3243(J/mol K). The degree of cure must to be zero at the die inlet and a temperatura de entrada (surrounding air) at 30 °C. The pull-speed was maintained at 2.299 mm/s for both cases study 1 and 2. The desired α must be 0.9, this is the target value of the mean degree of cure for the optimization. The die-cooler was maintained at 50 °C.

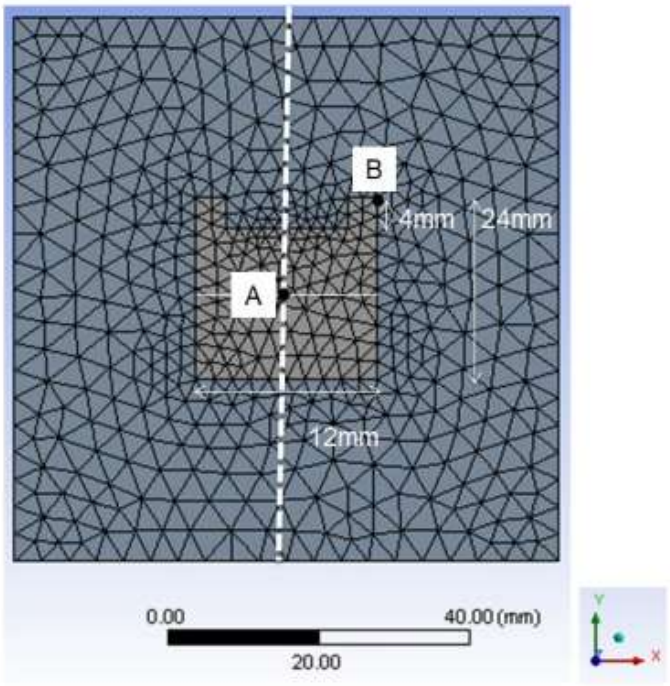

Fig.25. FE model of pultrusion die for the composite C-section.

Table 1
Materials and material properties used in the simulation [59]

Material	Density ρ (kg/m^3)	Specific heat C_p (J/Kg K)	Thermal conductivity k (W/m K)
EPON 20/9470/537 Epoxy resin	1260	1255	0.21
Glass fibers	2560	670	11.4
Crome (5%) steel	7833	460	40

4.2. Results (Validation Case)

The profile of the cross section of degree of cure and Temperature is shown in (Fig.22).The comparison between the results of the present analysis with the results reported in [59] is presented in Table 2. The results show that the procedure performed for the simulation is numerically valid (see Fig.26).

Table 2
Case Study 1 - Simulation results

Data	Pull Speed (mm/s)	Heater Temperature (°C)	Degree of cure	Temperature peak (°C)
Ref. [45]	2.299	105.5-148.5-200 115-146.5-200	0.875	218.0
Simulation	2.299	105.5-148.5-200 115-146.5-200	0.862	211.8

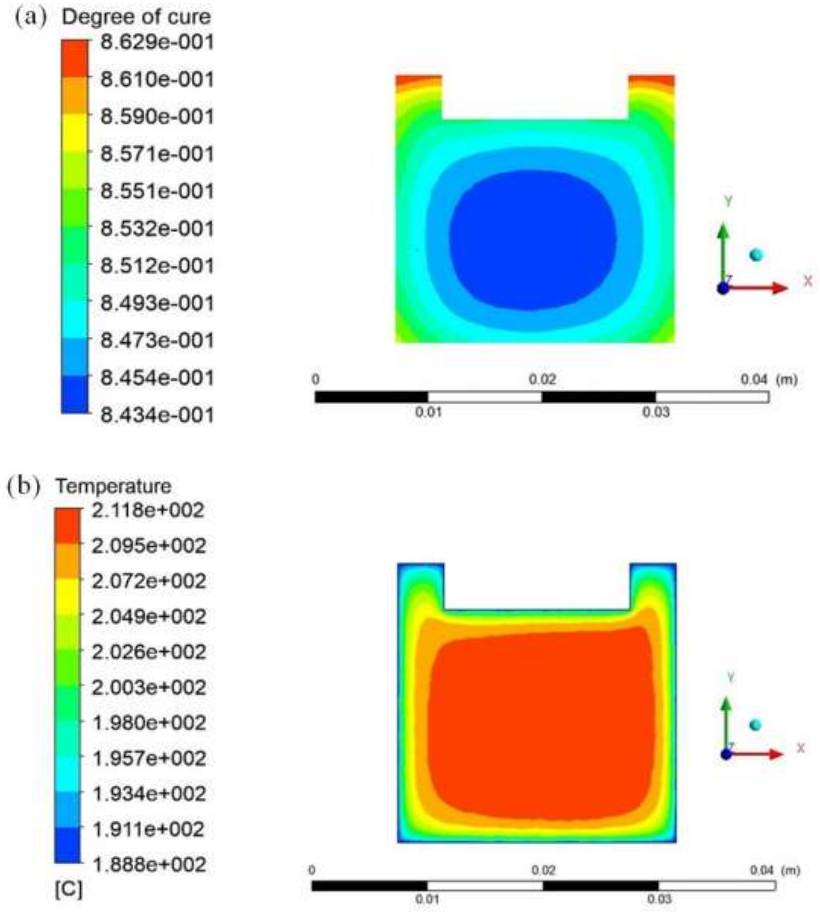

Fig.26. Profile of the cross section of temperature (a) and degree of cure from simulation (b).

4.3. Results Case Study 2 (C-section)

In this case, the numerical results obtained using the three algorithm, Matlab Quadratic Programming implementation (QP), Particle Swarm Optimization (PSO) and lLOG-Cplex Quadratic Programming implementation (CPX) are discussed.

The Fig.27 show the results of optimization study the degree of cure where (α) was assumed to be between (0 and 1). In this image there is (red) boundary line which represents the temperature within the die which cannot exceed the limiting temperature of 240 °C.

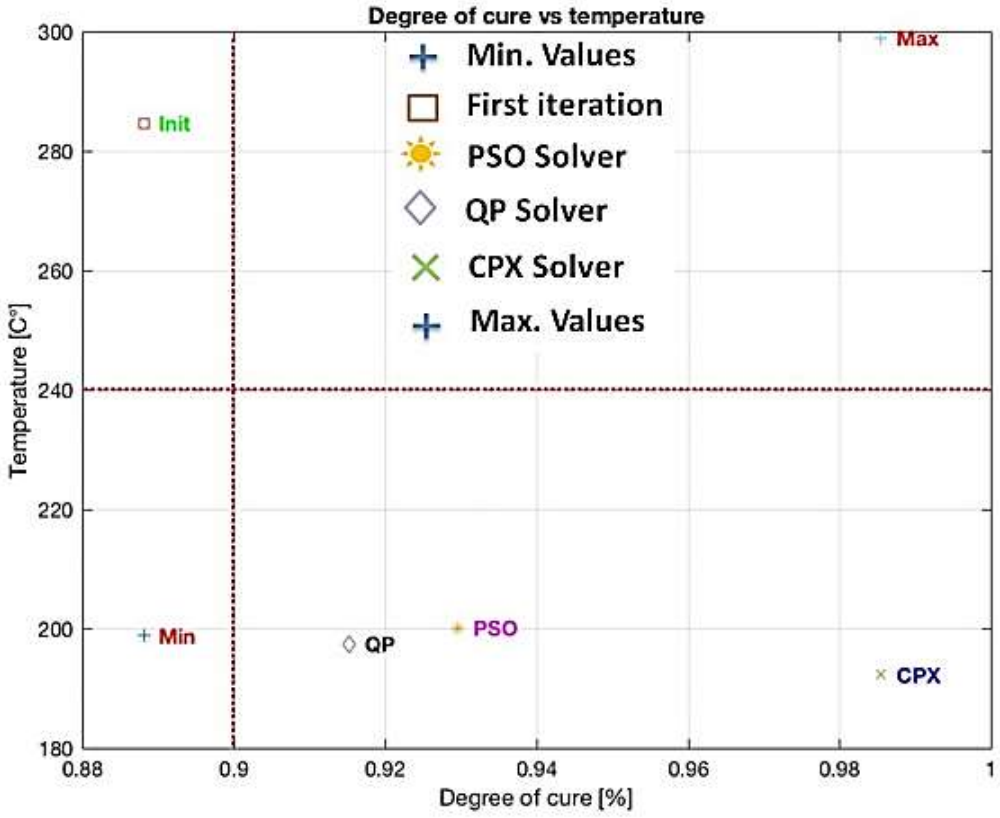

Fig.27. Mean degree of cure and temperature at die exit for three algorithms.

The results from optimization of pultrusion system show that (CPX) algorithm achieved an uniformity of degree of cure close to 98%. For the algorithm (PSO) the uniformity of cure was close to 94% and for (QP) was less than 92%. Analyzing temperature results, the temperature profile by CPX algorithm is more suitable because it leads to a better degree of cure.

4.4. Case study 3 (Internal Heaters)

The third case study aimed to simulate a pultrusion system with internal heaters using the input parameter temperature values from the optimization by algorithm (PSO) results. Thus, for this simulation was used kinetic parameters properties the same as in the firt case study, fibreglass and Shell EPON 9420/9470/537 epoxy resin (see Table 1). The third case study was carried out in order to compare (PSO) and (QP) algorithms.

4.5. Results (Internal Heaters)

The pultrusion system was simulated for a geometry with internal heaters in order to validate the numerical implementation for distinct die composite. It was simulate an arrangement of sixteen internal heaters with the temperature settings found in optimization by PSO algorithm, presented in (Table 3) and QP algorithm (Table 4).

The results present that the temperature of all the heaters does not contravene the maximum acceptable temperature of 240 °C. Contrarily, it can be noticed that the temperature regularly grows along the die length, achieving a maximum value in the middle of the gel zone (die).

Table 3
Internal heaters temperatures after optimization PSO (°C)

T1	**T2**	**T3**	**T4**	**T5**	**T6**	**T7**	**T8**
227	223.71	226.81	226.73	226.5	199.86	226.82	173.21

T9	**T10**	**T11**	**T12**	**T13**	**T14**	**T15**	**T16**
226.02	226.84	227	226.85	226.99	182.73	135.82	226.3

Table 4
Internal heaters temperatures after optimization QP (°C)

T1	**T2**	**T3**	**T4**	**T5**	**T6**	**T7**	**T8**
226.88	226.96	226.96	226.46	226.46	226.46	159.30	172.50

T9	**T10**	**T11**	**T12**	**T13**	**T14**	**T15**	**T16**
226.77	226.87	226.85	227.00	226.93	198.03	192.69	221.85

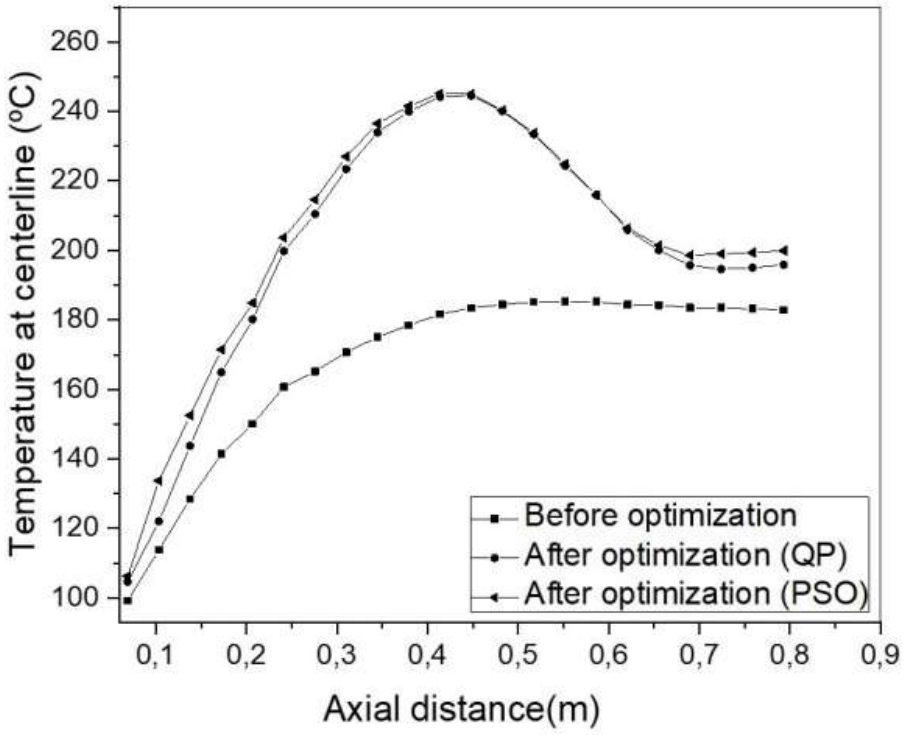

Fig.28. Predicted temperature at die exit found by (QP) and (PSO) algorithms.

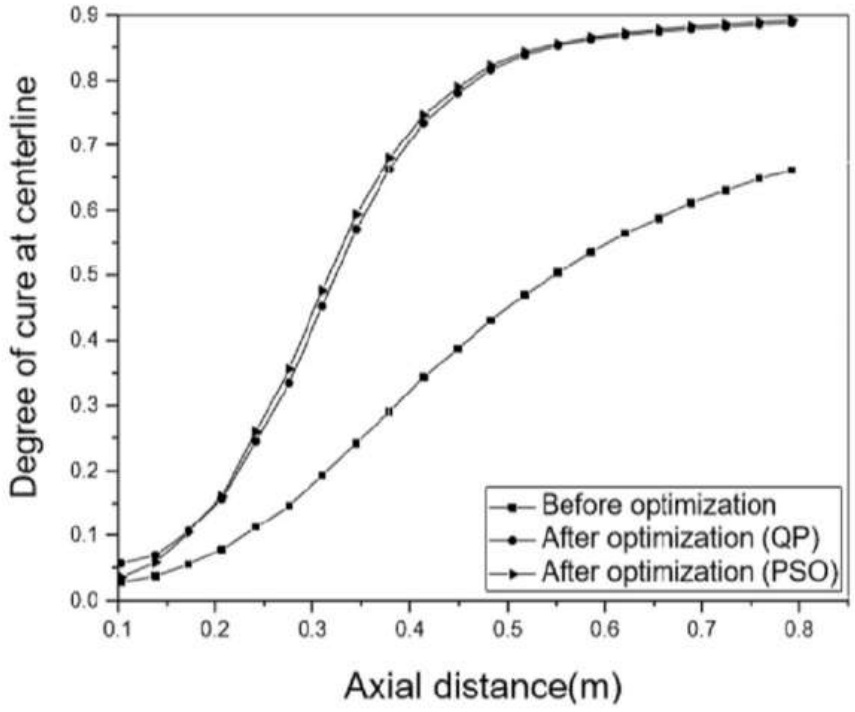

Fig.29. Predicted temperature at die exit found by (QP) and (PSO) algorithms.

It is possible see in Fig.28 the temperature is continuously reduced as the composite is formed (last zone). Note that the temperature profiles of top and bottom heaters are distinct. The degree of cure profiles and temperature profile is see in the figures (Fig. 28) and (Fig.29), respectively. The optimal degree of cure at the die exit was approximately 0.9 for both algorithms.

Results from algorithms (QP) and (PSO) show roughly the same values for the degree of cure, 0.891 and 0.895, respectively (see Table 5). Concerning the temperature, the optimization with (PSO) resulted in a temperature of the composite was 211 °C whilst with (QP) the temperature was 200 °C.

The relative dissimilarity between the results of (PSO) and (QP) can be explained by the fact that (QP) is an exact algorithm while (PSO) is just a meta-heuristic. The Particle Swarm Optimization bid to improve the current appropriate solution at each repetition (see Fig.30 and Fig.31).

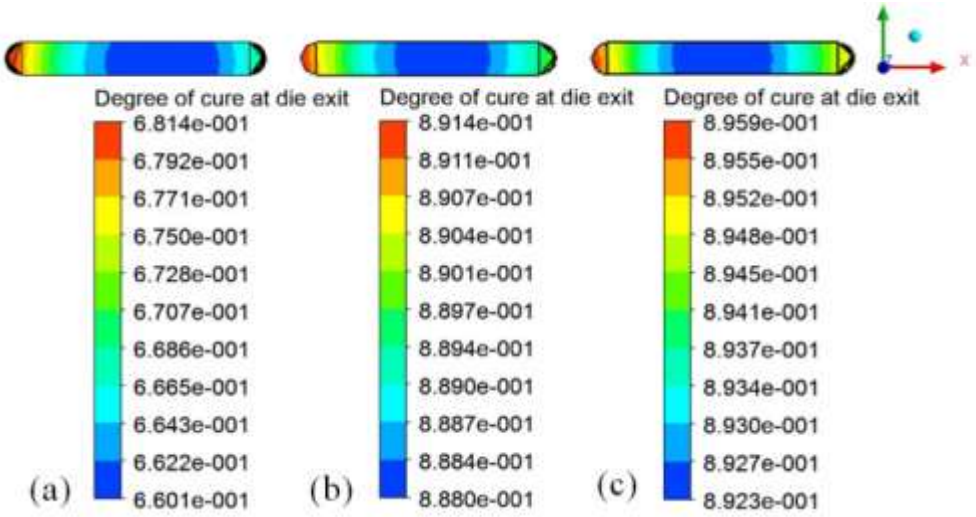

Fig.30. Degree of cure profiles before optimization (a), optimization by Quadratic Programming implementation (b) and Particle Swarm Optimization (c).

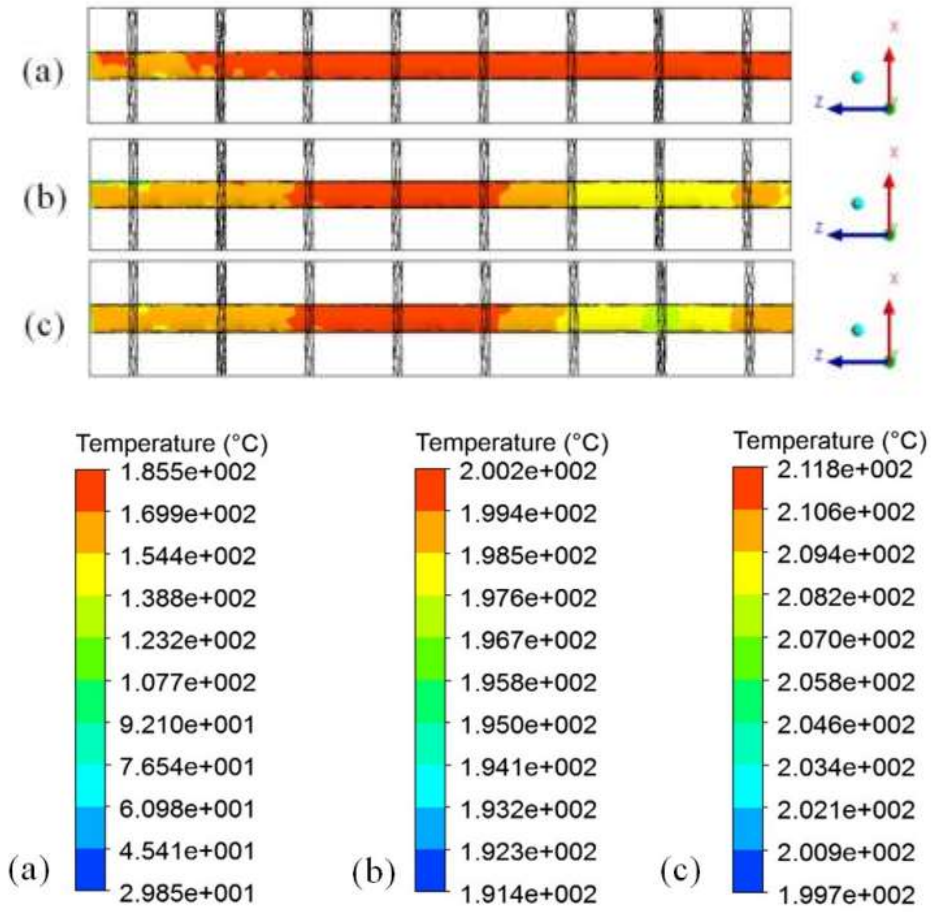

Fig.31. Temperature profile before optimization (a), optimization by Quadratic Programming implementation (b) and optimization by Particle Swarm Optimization.

Table 5
Comparison results

Data	Temperature (°C)	Degree of cure at die exit	Pull-speed (mm/s)
Before optimization	182.9	0.6814	5.00
After optimization PSO	203.5	0.8959	5.00
After optimization QP	200.2	0.8914	5.00

Three different algorithms were used to analyze the temperature setting of matrix heater on pultrusion process with the objective to improve the cure rate and reach to the value (0.9). Results from the second case study show ILOG-Cplex Quadratic Programming implementation algorithm was adequate showing 0.98% of cure.

Results from third case study presented the validation of the numerical implementation for different die-composite. Thus it is possible to see that the degree of cure can be improved for all the algorithms used in this study, however the particular Swarm Optimization shows satisfactory results granting a betther temperature settling for the pultrusion process thus offering positive results to ensure the quality of composite material.

5. Methodology (Kinetic Model)

5.1. Experimental procedure

The materials used in this study were purchased from Exel Composites GmbH company (Austria) and stored at room temperature. An epoxy resin derived from an unmodified liquid diglycidyl ether of Bisphenol A (DGEBA resin) in a mixture with an Anhydride Curing Agent and an Accelerator like DMP-30 (2,4,6-tris(dimethylaminomethyl) phenol) was characterized. Based on these arguments, the suggested curing mechanism, used to represent the cure kinetic is represented. For the Differential scanning calorimetry (DSC) measurements the (Mettler-Toledo DSC) was used, reagent mixtures were prepared at a mass ratio of 100 : 85 and 1.60 phr (hundred parts resin) accelerator content. The system was cured under non-isothermal conditions at heating rates of 2,5,10 and 15 °C/min over a temperature range of 25°C to 250°C. Samples of 4 mg were examined in pierced aluminum pans sealed under nitrogen atmosphere.

Heat flux-temperature profiles were determined by calculation and experiment for a cylindrical sample of 4 mg. In the DSC experiment, starting with fresh uncured resin, the sample was scanned at a selected heating rate from room temperature up to a temperature at which the reaction was complete. After the resin has been given a precure, it was cooled and then scanned under conditions close to the initial conditions, to give the reference baseline.

5.2. Parameter estimation of empirical model

The method employed in this study based on dynamic DSC analysis.

Complete the results achieve from DSC measurements, it was possible to determine the kinetic parameters of the resin reaction by the Kissinger method. The (Tp) peak temperature, change to a higher temperature range with increasing (β) heating rate [69]. Hence, the Kissinger [69,70]. method can be employed to calculate the activation energy of the cure of epoxy resin [71].

The Kissinger method is the most common approaches to detect kinetic parameters by thermal analysis. The exothermic peak temperature (Tm),

is a point of constant change, it is measured for each heating rate. The Kissinger method considers a first order equation by peak temperature at a data point for each heating rate. The equation for the Kissinger method can be defined as:

$$\ln\left(\frac{\beta}{T_p^2}\right) = \ln\left(\frac{AR}{E_\alpha}\right) - \frac{E\alpha}{RT_p} \tag{29}$$

where the R is the universal gas constant. E_a is the activation energy, A is the pre-exponential factor and the peak temperature, T_p, exchange to a higher temperature range with increasing heating rate, β.

The activation energy is obtained by plotting $\ln\left(\frac{\beta}{T^2}\right)$ versus $\frac{1}{T_p}$, and the values of activation energy, A, and pre-exponential factor, E_a, is predicted by calculating the slope of the linear fit and the y-intercept [69, 72].

5.3. Parameter estimation: Optimization

The approach to estimate the parameters of the kinetic models was established on the optimization of the mean square deviation between the degree of experimental and theoretical curing obtained at different temperatures. As mentioned in the previous topic, four heating rates were used: 2, 5, 10, 15 and 20°C/min. In this way, the objective function is defined by the following equation [62]:

$$F = \sqrt{\sum_{i=1}^{N_j} (\alpha_i - \alpha_i^*)^2} \tag{30}$$

In which α is the degree of cure, N_j is the size of each j_{th} data and F is the objective function to be minimized. For each case, a parametric optimization was performed, in which the objective was minimizing the deviation between the experimental degree of cure $(\alpha)^*$ and the values predicted by the model (α), regarding different temperature rates, at each point i of a dataset $N_j, j = 1,...,4$.

Thus, the optimization problem can be formulated according to:

$$\min\left[F=\sqrt{\sum_{i=1}^{N_j}(\alpha_i-\alpha_i^*)^2}\right] \tag{31}$$

Subject to:

$$\frac{\partial\alpha}{\partial t}=A_0\exp\left(-\frac{E_a}{RT}\right)(1-\alpha)^n \tag{32}$$

$$A_0,\min \le A_0 \le A_0,\max \tag{33}$$

$$n_{\min} \le n \le n_{\max} \tag{34}$$

Thus ($\min$) and ($\max$) are the minimum and maximum values of the optimization algorithm respectively. The bounds for the independent variables were fixed according as $A_0,\min=0.01$, $A_0,\max=1.10^6$, $n_{\min}=0.01$ and $n_{\max}=4$.

5.4. Phenomenological kinetic model

$$\min\left[F=\sqrt{\sum_{i=1}^{N_j}(\alpha_i-\alpha_i^*)^2}\right] \tag{35}$$

$$\frac{dA}{dt}=-k_1[A][B]+k_1^*[C] \tag{36}$$

$$\frac{dB}{dt}=-k_1[A][B]+k_1^*[C] \tag{37}$$

$$\frac{dD}{dt}=\frac{dG}{dt}=-f.\frac{k_1k_2}{k_1^*}[A][B][D] \tag{38}$$

$$f=\frac{1}{1+e^{(C.(\alpha-\alpha_C))}} \tag{39}$$

$$\alpha = 1 - \frac{[G]}{[G_0]} \tag{40}$$

$$k_i = A_0, ie^{(-E_a, i/RT)}, \; i = 1,..3 \tag{41}$$

And the following bounds:

$$A_0, i, \min \leq A_{0,i} \leq A_0 i, \max \tag{42}$$

$$E_a, i, \min \leq E_{a,i} \leq E_a i, \max \tag{43}$$

$$C \min \leq C \leq C \max \tag{44}$$

$$\alpha_c \min \leq \alpha_c \leq \alpha_{c,} \max \tag{45}$$

The ($\min$) and ($\max$) are the minimum and maximum values of the optimization algorithm respectively. The bounds for the independent variables were fixed according as $A_0, i, \min = 0.01$, $A_0, i, \max = 1.10^6$, $E_a, i, \min = 100$, $E_a, i, \max = 1.10^6$, $C \min = 0.01, C \max = 20$, $\alpha_c, \min = 0.01$ and $\alpha_c, \max = 0.95$.

In order to solve the ordinary differential equation (ODE) system represented by Equation (11), the 4th Runge-Kutta method (ode45) was implemented throughout the use of Matlab® software. The particle swarm algorithm (PSO) [26,74] was used to minimize the least square deviation function.

The simulation target to predict the variation of temperature and degree of cure regarding a three-dimensional piece. In this model, mass and energy balances, (Equations 1, 2 and 3) were considered to study the thermal and kinetic behavior and degree of cure of pultrusion process. therefore, the control volume worn for such procedure was the mold region (Pultrusion die, see Fig.32).

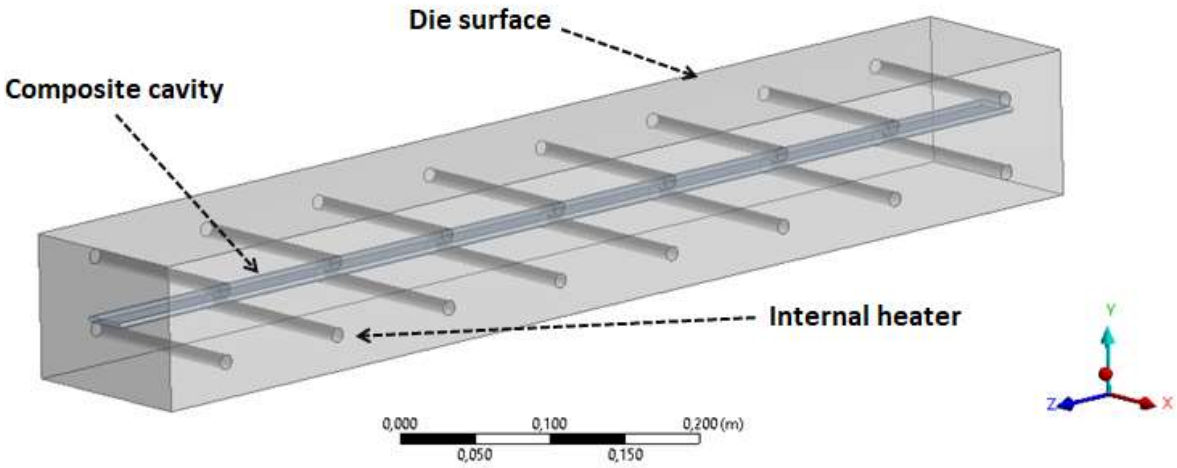

Fig.32. Predicted temperature

The details of the composite part are illustrated in the Fig.33. In order to solve the pultrusion process, the Finite Volume Method, configured into Ansys CFX Solver®, was used. After some numerical tests, the pieces mesh was generated by the use of the software Ansys Meshing®, as shown in Fig.34. It resulted in 60247 elements and 92596 nodes. The list of physical properties (Glass fiber [26,74] and Epoxy resin) are disclosed in Table 6.

In the simulation, the degree of cure is to be zero at the entrance and the resin feed temperature must be the environment temperature:

$$T_{Z=0} = T_0 = 25°C \tag{46}$$

$$\alpha_0 = 0 \tag{47}$$

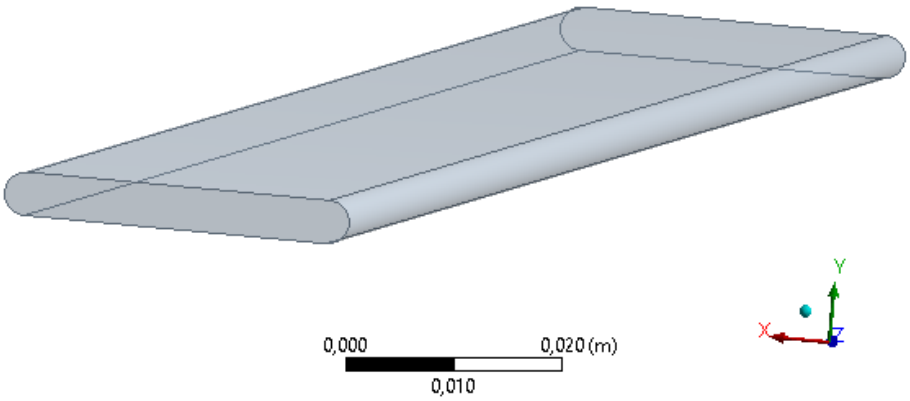

Fig.33. Design of composite part.

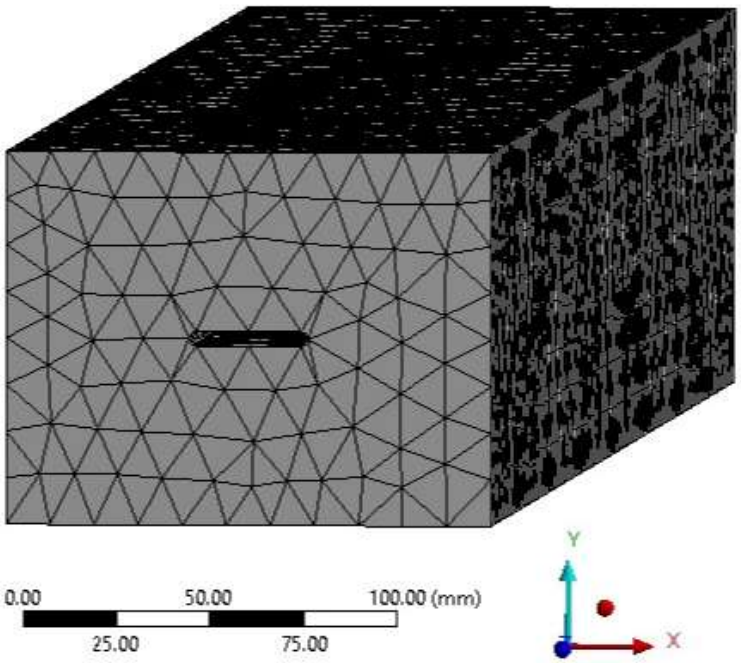

Fig.34. Mesh generation into Ansys Meshing®

Table 6
Physical properties (Based on [26,74])

Property	Description	Value
Φ_r	Resin volume fraction	0.55
Φ_f	Fiber volume fraction	0.45
ρ_r	Resin density	1150 $kg.m^{-3}$
ρ_f	Fiber specific heat	2560 $kg.m^{-3}$
k_r	Resin thermal conductivity	0.169 $J.m^{-1}.s^{-1}$
k_f	Fiber thermal conductivity	1.04 $J.m^{-1}.s^{-1}$
$c_{p,r}$	Resin specific heat	1640 $J.kg$-1.K^{-1}
$c_{p,f}$	Fiber specific heat	640 $J.kg.m^{-3}$
$C_{a,0}$	Feed resin mass concentration	1100 $kg^{-1}.K^{-1}$
T_H	Temperature of the heaters	500 K
w	Pulling speed	0.005 $m.s^{-1}$

The calculation to find the physical properties of the composite is presented in successive equations below.

$$\rho_c = \phi_r \rho_r + \phi_f \rho_f \tag{48}$$

$$\rho_c c_{p,c} = \phi_r \rho_r c_{p,r} + \phi_f \rho_f c_{p,f} \tag{49}$$

$$\frac{1}{k_c} = \phi_r \frac{1}{k_r} + \phi_f \frac{1}{k_f} \tag{50}$$

5.5. Methodology - Flowchart

The flowchart of the procedure of this work is illustrated in Fig.35. In the first step, the curing degree curve is obtained in the DSC analysis at different heating rates.

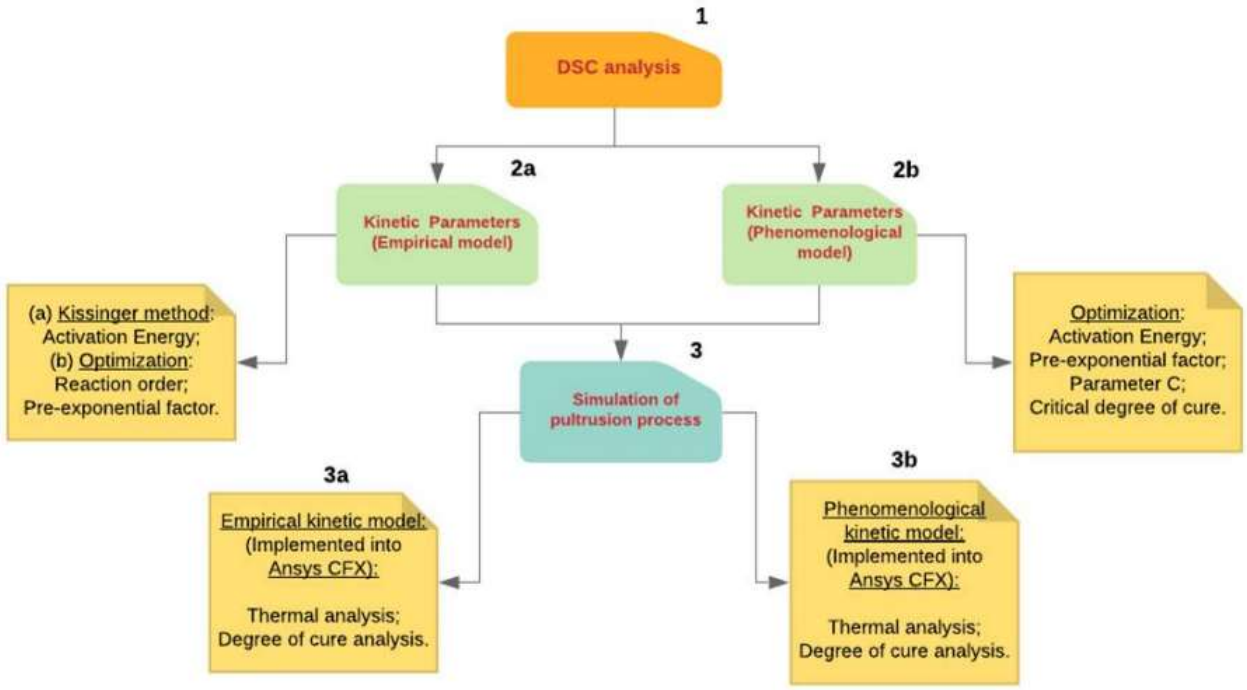

Fig.35. Summary of methodology

These data are collected for later adjustment of the kinetic parameters. The second step consists in estimating the kinetic parameters with the data obtained in the step 1. In this case, as explained previously, two kinetic models were used: (2a) empirical model and (2b) phenomenological model. In the empirical model, the Kissinger method was used to estimate the activation energy, while the other parameters were estimated through the optimization procedure. In the phenomenological model the optimization was also used. In the third step (3), the pultrusion process was simulated according to the kinetic models obtained. The temperature and curing profiles were evaluated. The optimization procedure is outlined in Fig.36.

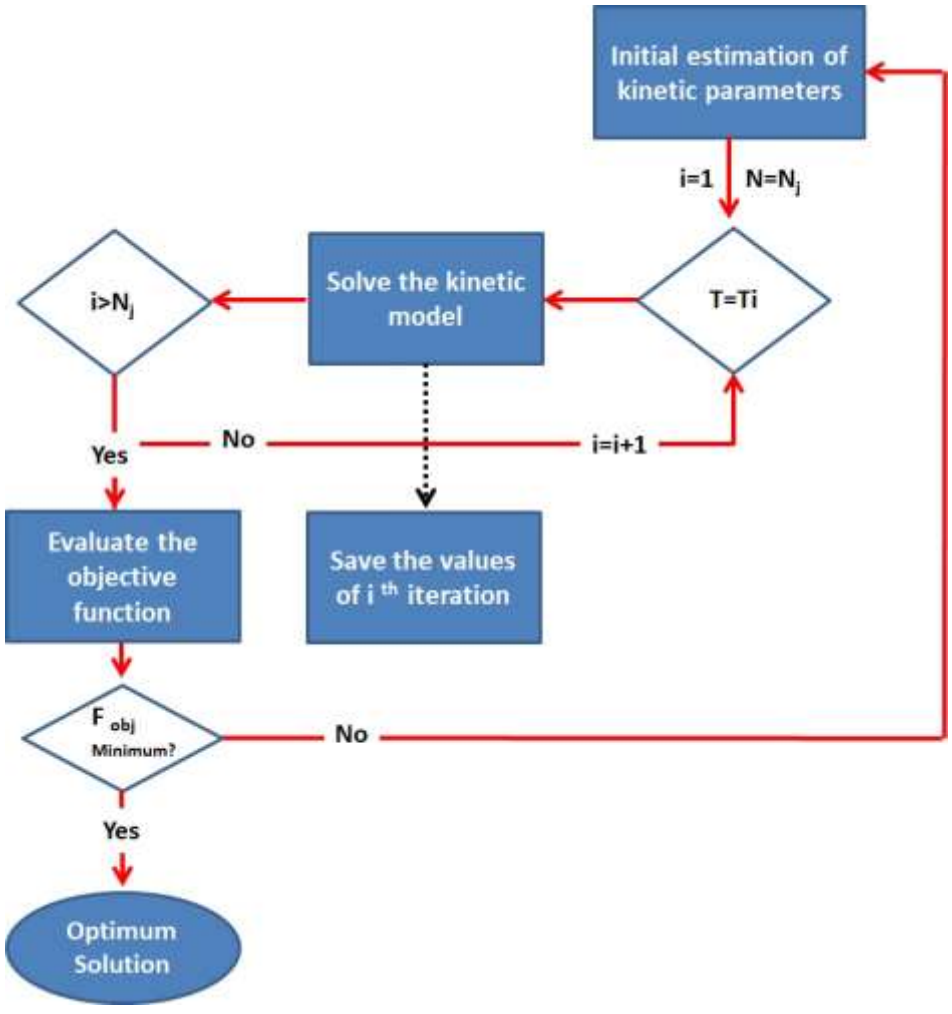

Fig.36. Summary of the optimization procedure.

6. DSC analysis and Parameter estimation of empirical kinetic model parameterstion

6.1. Results of DSC analysis

The Fig.37 shows the results of DSC analysis. According to the results of Figure 34, the shape and position of the heat flux-temperature curve may depend on the value selected for the heating rate due to the changes in temperature within the sample. This change is caused by the heat transferred by conduction and the heat generated by the curing reaction. As shown, the curve peaks are shifted towards a higher temperature when the heating rate is enhanced. As a consequence, too high value can be obtained for the activation energy, as well as for the pre-exponential factor.

During a non-isothermal curing process, the heat flux was monitored over time and the basic hypothesis for data analysis is that this heat flux is proportional to the reaction rate. Therefore, the total reaction heat is calculated as being proportional to the area of the curves (represented by the Fig.38). Notice that, the heating rate must be taken into account to calculate the reaction heat, according to the following equation:

$$\Delta H = \frac{1}{m_s}\int_0^{t_f} Q(t)dt \tag{51}$$

in which ΔH is the reaction heat m_s is the sample mass, t_f is the final time and $Q(t)$ is the heat flux.

According to our analysis, the average heat flux was 398.3 *J/g*. However individual values could be obtained: 405.4 *J/g, 391.9 J/g, 398.2 J/g and 403.7 J/g* for 2, 5,10 and 15°C/min, respectively.

It is possible to observe that the degree of cure increases with temperature, as expected, for different heating rates. The results show that curing occurs faster for high heating rates, but in all profiles, it was possible to reach maximum cure at the temperature of 250°C. The image of the cured resin shown in Fig.39.

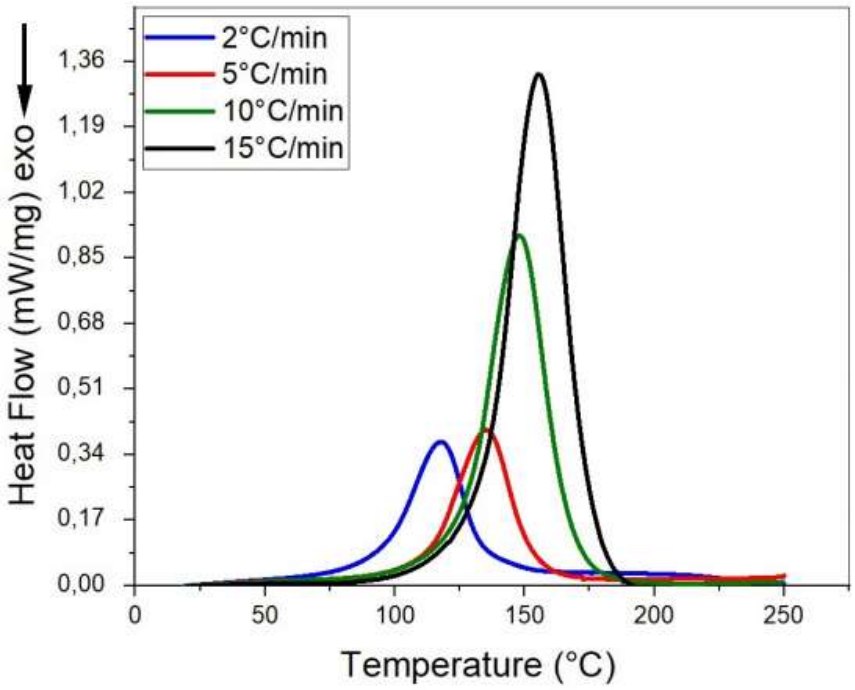

Fig.37. The evolution of heat flow for the dynamic DSC experiments.

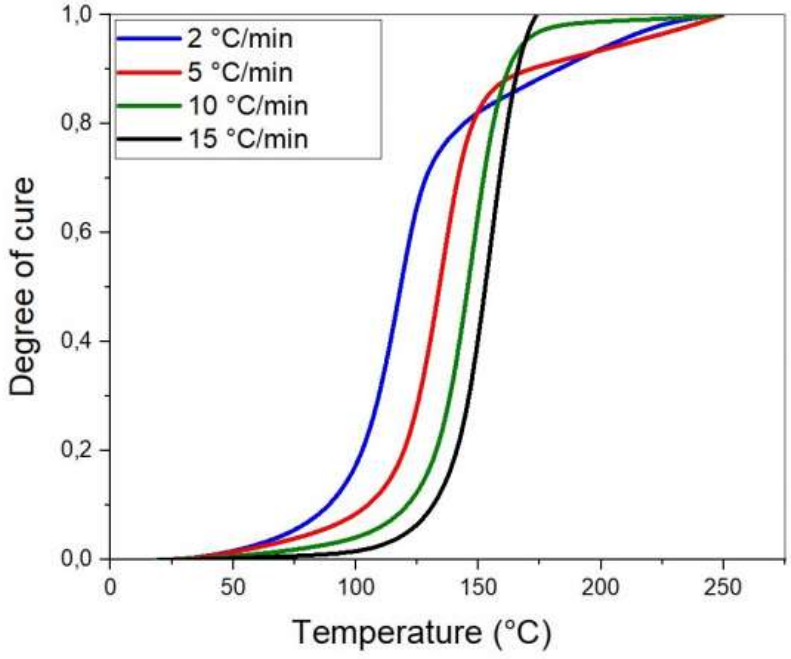

Fig.38. The evolution of degree of cure for the dynamic DSC experiments.

Fig.39. Epoxy resin derived from an unmodified liquid diglycidyl ether of Bisphenol A (DGEBA resin) in a mixture with an Anhydride Curing Agent and an Accelerator like DMP-30 (2,4,6-tris(dimethylaminomethyl) phenol.

6.2. Parameter estimation of empirical kinetic model parameters

In order to estimate the kinetic parameter values of the empirical model, the Kissinger [69] method was used to compute the activation energy, and the optimization was used to compute the other kinetic parameters (A_0 and n).

The Fig.40 illustrates the adjustment resulted from the Kissinger method. According to the results obtained by the interpolation, the activation energy was 63.717 *kJ/mol*.

In this division of study, the method to estimate the kinetic parameters from the experiment conducted at 5 °C/min will be explained. The (Fig.41) show the degree of cure profile obtained for the heating rate of 5°C/min. Notice that a greater deviation was verified for temperature values higher than 150°C, indicating that the

kinetic model tends to deviate from the experimental results for this temperature range.

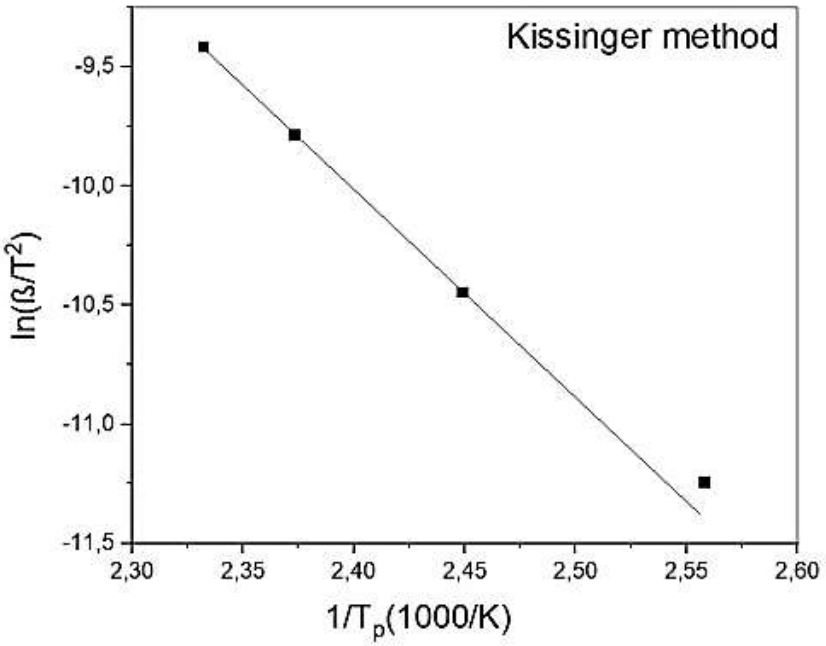

Fig.40. Kissinger's plot to determine activation energy (E_a).

The results of parameter estimation by considering the diffusional effects are reported in Table 7, in which the diffusive parameters *C* and α were also included as independent parameters into the optimization procedure.

In Table 8, *n* is the reaction order, *F* denotes the objective function and *N* is the number of experimental data. As seen, different values of specific total enthalpy were obtained: 405.4 J/g, 391.9 J/g, 398.2 J/g and 403.7 J/g for 2,5, 10 and 15°C/min, respectively. It is noted that the values are relatively close, presenting an average value of 399.8 J/g and a standard deviation of 6.09 J/g. The enthalpy variation can be explained by several factors, such as experimental errors or even the influence of the heating rate on the specific total enthalpy, as observed by Vergnaud and Bouzon (2011) [75].

An optimization study encompassing all the experimental points (global case) was also accomplished. The results are shown in the last line of Table 8. As can be seen, the optimization gave satisfactory results, with F equals to 1.701. Besides, the

values of the kinetic parameters were in the same order of magnitude as the values presented by the other cases. It is important to emphasize that, for the global case, the specific total enthalpy could not be obtained, since it is computed experimentally by the DSC instrument. Thus, for the simulation of pultrusion process, the average H_r was used, as explained in the next topic.

Table 7
Bounds of kinetic parameters.

Parameter	Bounds	
	min	max
K_0	1.10^2	1.10^6
n	0.01	4
E_a (J/mol)	1.10^2	1.10^6
C	0.01	120
α_c	0.5	1.0

Table 8
Kinetic parameter and objective function for heating rate of 2, 5,10 and 15°C/min.

Heating rate	E_a (*kJ/mol)*	*n*	$k_0(s^{-1})$	*F*	*N*	*Hr (J/g)*
2°C/min	63.717	2.039	548,571	3.028	6,874	405.4
5 °C/min	63.717	1.210	459,497	2.293	2,761	391.9
10 °C/min	63.717	0.587	426,577	1.595	1,386	398.2
15 °C/min	63.717	0.588	426,582	1.696	920	403.7
Global	63.717	0.682	427,562	1.791	10,931	--

The results of objective function indicate that a good adjustment could be obtained for the four case studies, in which an average improvement of objective

function in relation to the previous results (Table 9) was 19.55% (regarding the four heating rates). The standard deviation of reaction order (*n*) and frequency factor (k_0) were 0.79 and $8.601.10^4$ s^{-1}, respectively. These results can be interpreted in Fig. 41, which shows the comparison between the curing profiles of both empirical models.

Table 9
Kinetic parameter and objective function for heating rate of 2, 5,10 and 15°C/min (by the inclusion of diffusional effects)

Heating rate	E_a (*kJ/mol)*	*n*	$k_0(s^{-1})$	*F*	*C*	*F(%)*
2°C/min	63.717	1.945	548,572	2.620	14.41	-13.47
5 °C/min	63.717	1.02	459,481	1.591	78.89	-30.61
10 °C/min	63.717	0.121	338,738	1.287	76.93	-19.31
15 °C/min	63.717	0.494	456,259	1.445	19.99	-14.79
Global	63.717	1.03	457,268	1.486	19.73	-16.13

The results of the optimization applied to all experimental data set (global case) are shown in the last line of Table 8. As observed, a slight decrease of the objective function, in relation to the previous global-case of Table 9, was observed, with a relative decrease of *F* equals to 16.13%.

The results of Fig.41 show that the quality of fit was better for the diffusional empirical model. Notice that a smaller error could be obtained for high values of degree of cure, indicating that the diffusional parameter is capable of improving the optimization in this stage. Such a result can be explained by the fact that the diffusion control occurs at higher conversions due to the increase in the viscosity of thermoset matrix, which reduces reaction rate.

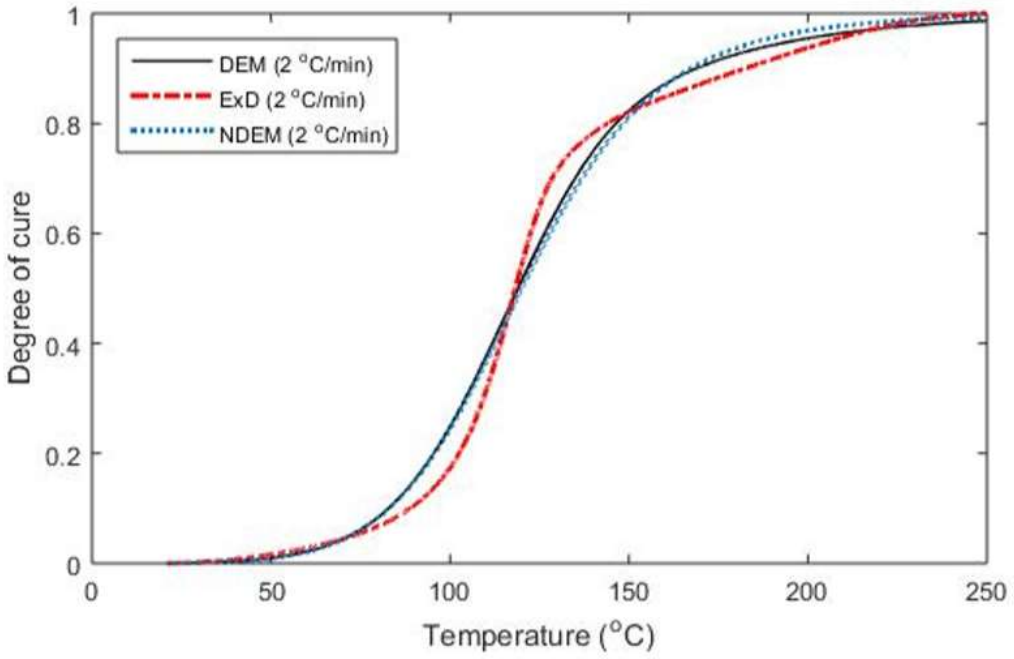

(a) 2°C/min

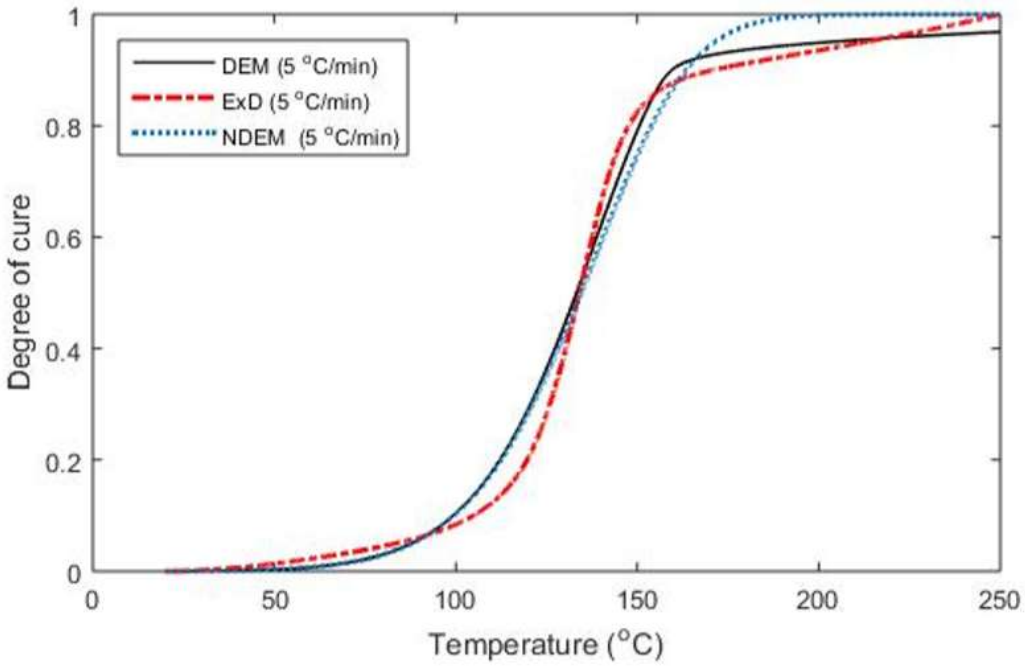

(b) 5°C/min

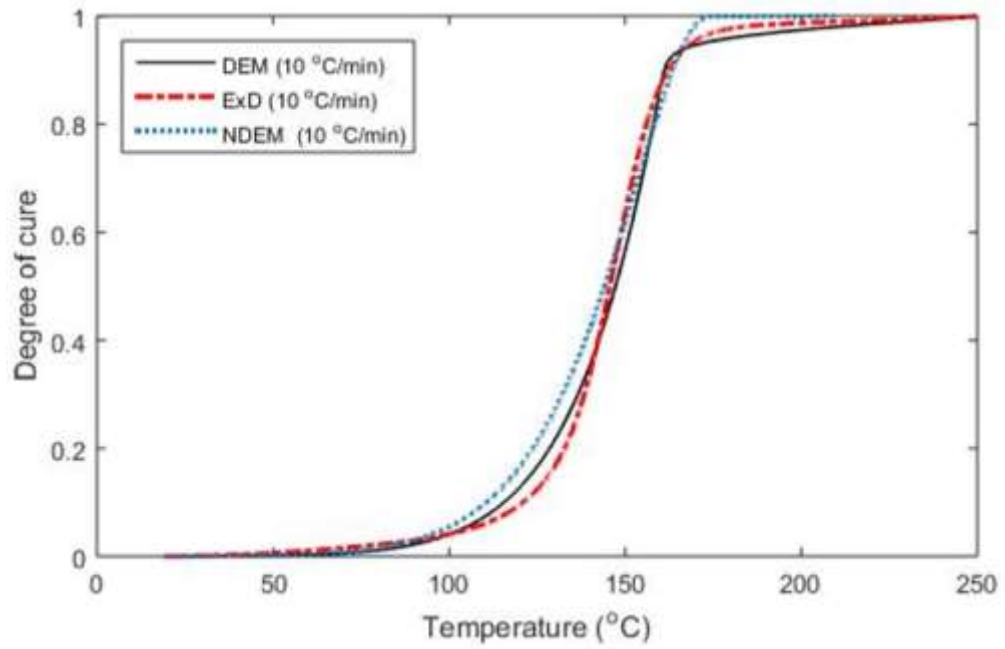

(c) 10°C/min

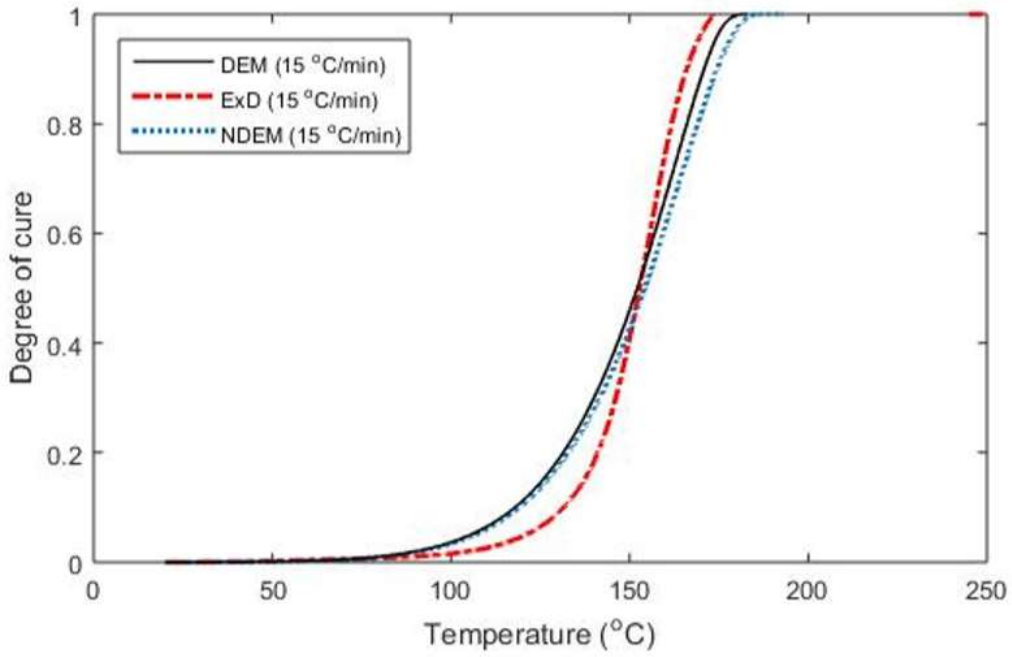

(d) 15°C/min

Fig.41. Simulated and experimental curing profiles for 2, 5, 10 and 15°C/min (dark curve: diffusional empirical model (DEM); traced curve: experimental data (ExD); dot curve: non-diffusional empirical model (NDEM).

6.3. Results: Parameter estimation with the phenomenological model

As said previously, the optimization procedure was also applied to the phenomenological model developed from the phenomenological model, based on the works of Antoon et al. [44] and Corsetti et al. (2013) [67]. In this case, only the diffusional term was considered, since the advantages of implementing it to predict the curing reaction of epoxy resins have been evidenced recently [70,76,49] and also demonstrated in the last section for the analysed system.

The results of the optimization are summarized in Table7 in which the values of the kinetic parameters: $E_{a,i}, k_{0,i}, C, \alpha_c$ and *F* are reported for each heating rate.

Table 10
Kinetic parameter of the phenomenological model

Parameter /Heating rate	2°C/min	*5°C/min*	10°C/min	*15°C/min*	*Global*
$E_{a,1}$ (kJ/mol)	$9.114.10^4$	$9.454.10^4$	$9.812.10^4$	$9.724.10^4$	$7.676.10^4$
$E_{a,2}$ (kJ/mol)	$1.636.10^3$	$2.372.10^3$	$9.434.10^3$	$2.413.10^3$	$2.876.10^3$
$E_{a,3}$ (kJ/mol)	0.021	0.017	0.032	0.027	0.021
$K_{0,1}$ (s^{-1})	$7.594.10^4$	$3.774.10^4$	$3.059.10^4$	$1.094.10^5$	$4.567.10^5$
$K_{0,2}$ (s^{-1})	$6.356.10^4$	$3.878.10^3$	$7.321.10^3$	$2.277.10^3$	$6.433.10^4$
$K_{0,3}$ (s^{-1})	1.201	0.984	0.958	0.971	0.966
C	16.901	16.38	23.301	6.092	27.4
α_c	0.668	0.705	0.996	0.954	0.956
F	2.126	1.360	1.166	1.180	1.318
$\delta F(\%)^9$	-18.85	-14.51	-9.40	-18.33	-11.31

As seen, an average improvement of the objective function equals to 15.25% was obtained, in relation to the result of the diffusional empirical model. This indicates that the proposed model provided parameters of good quality for predicting the curing reaction. Notice that the maximum *F* decrease of 18.85% was observed for 2°C/min (see Table 10), with the objective function value of 2.126. In addition, the global estimation was also performed, with the relative improvement of 11.31 %. It should be noted that the value of $k_{0,3}$ and $E_{a,3}$ presented an order of magnitude significantly lower than the other values, denoting that the reverse reaction is not favorable.

The curing degree profiles obtained with the phenomenological model are displayed in Fig. 42. On the whole, it is possible to see that the curves of empirical and phenomenological models follow similar trends, however, it is clear that that a little improvement could be obtained with the application of phenomenological model.

The results indicate that the proposed approach can be satisfactory to model the kinetic behavior of the analysed epoxy resin system. Also, the inclusion of the diffusional term contributed to improving the adjustment of predicted curves to experimental data. Finally, it seems that, although the mathematical complexity increases with the use of the phenomenological model, the number of degrees of freedom of the optimization problem is higher, which may favor the parameter estimation methodology.

6.4. Results: Simulation of Pultrusion process

According to Vergnaud and Bouzon (2011) [75], the DSC, normally, low values of heating rates are chosen for evaluating the curing reaction because it avoids high temperature gradients during the experiment. As recommended by Vyazovkin et al.(2014) [34]., when nonisothermal measurements are used, it is recommended to begin the measurements with a slow heating rate (1°C/min) and use the data obtained as a reference for evaluating the quality of data at a higher heating rates. However, for the experiment executed in this work, the value of 15 °C/min, still gave good results, as observed previously. In spite of this, three of the

previous cases were chosen for the simulation of pultrusion: (i) heating rate of 2 °C/min, (ii) heating rate of 10 °C/min and (iii) global case.

The comparison between the solutions obtained with diffusional empirical and phenomenological models can be visualized in Fig. 42, in which the curing and temperature profiles in the center-line of the composite part were compared.

The results evidence that the curing profiles predicted by the proposed models presented a similar trends, indicating a gradual polymerization along the die length. The shape of the curing profiles, with a typical S-curve, are in accordance with the results of recent works [2,5,52] regarding pultrusion processes. It is noted that at degree of cure higher than 0.4 the deviations between the curves increases, which are in line with the previously results of parameter estimation. According to the results, the mean absolute errors were 0.591, 0.588 and 0.594 for 2 °C/min, 10 °C/min and global-case, respectively.

The temperature profiles, displayed in the Fig. 42 shows that the temperature change along the part is very similar for both models. The result evidences that there is a rapid increase in the temperature at the inlet of the die cavity due to the energy released during the curing reaction. The temperature passes through a maximum, and finally decreases in the final part. Regarding the temperature curves, the relative errors were 6.080, 4.358 and 7.287 and for the cases 2, 15 and global, respectively.

The presented results reveal that in all cases it was possible to obtain significantly close curing and temperature profiles. However, it is noted that the relative error between the two methods was somewhat less in the case of the heating rate of 10 °C/min, which also showed that the curve fitting result was in good agreement with the experimental data.

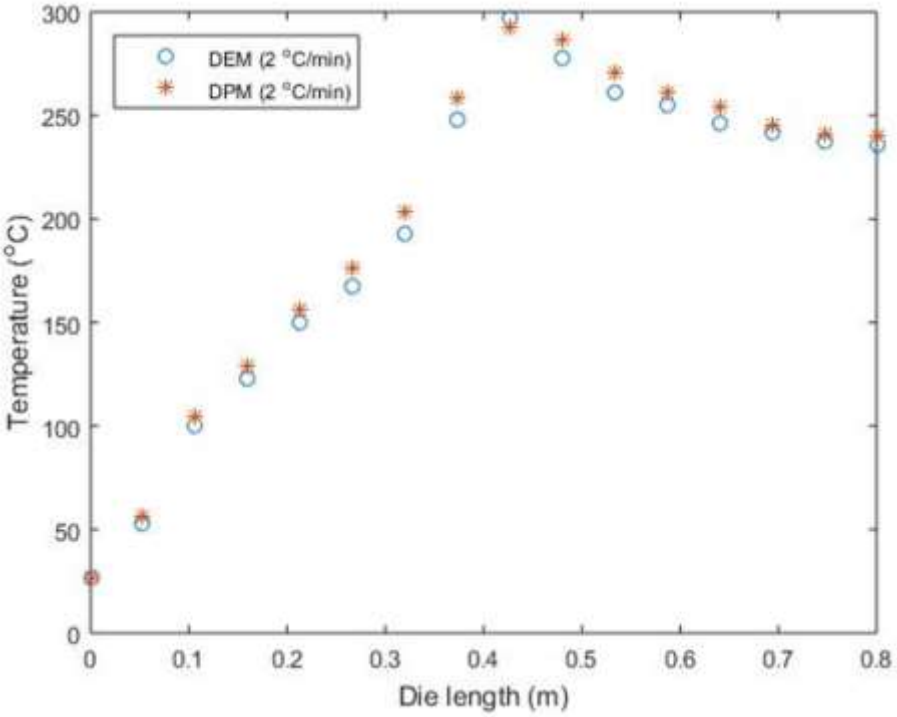

(a) 2°C/min

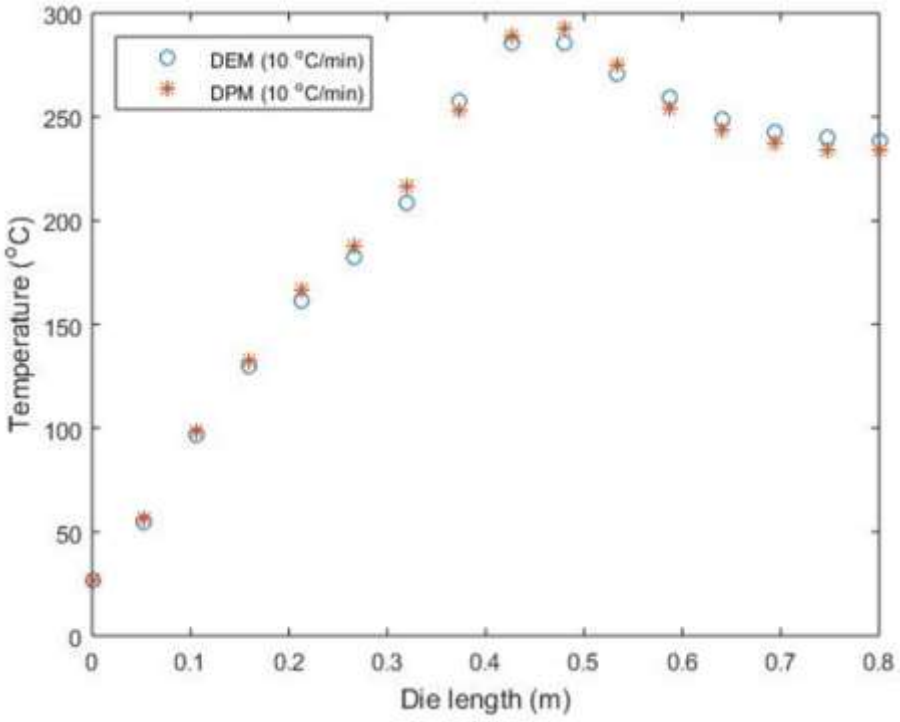

(b) 10°C/min

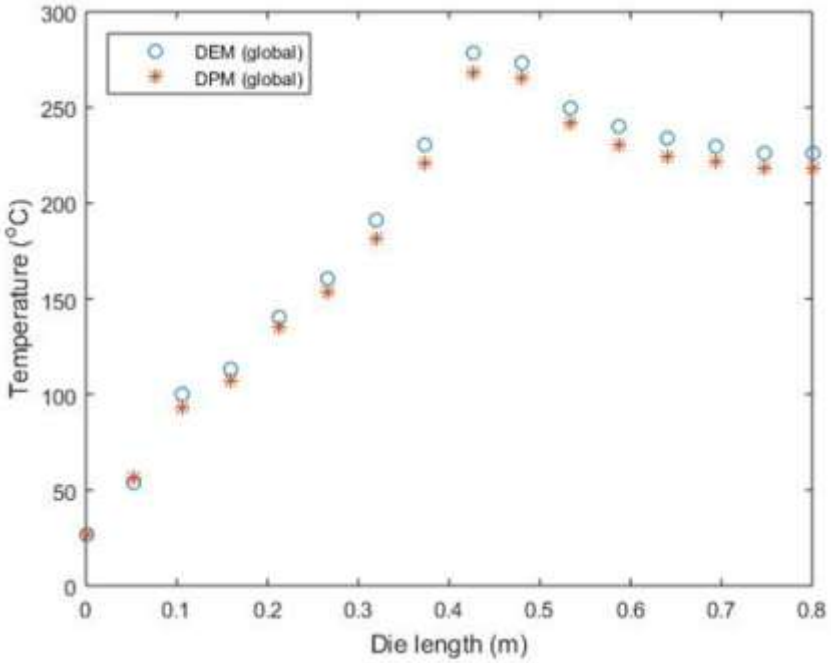

(c) Global

Fig.42. Simulated temperature profiles for 2 °C/min, 10 °C/min and global-case for diffusional empirical model (DEM) and diffusional phenomenological model (DPM).

7. Conclusions

In this doctoral work, we performed optimization of the pultrusion process using three different algorithms to identify an optimal temperature setting of heater (pultrusion die) leading to the best possible degree of cure. As shown by the case study 2, the algorithm (CPX) was able to find the best degree of cure, approximately to 0.98%.

In the third case study, results shown the validation of the numerical implementation for different die-composite. The degree of cure can be enhanced for all the algorithms used in this thesis, however the (PSO) presented positive results allowing a greater distribution of the temperature in the pultruded material.

The objective of the second stage of this doctoral work was to study the cure kinetic of an epoxy resin derived from an unmodified liquid diglycidyl ether of Bisphenol A (DGEBA resin) in a mixture with an Anhydride Curing Agent and an Accelerator like DMP-30 (2,4,6-tris(dimethylaminomethyl) phenol). The following steps were conducted:

(1) The kinetic parameters were calculated from the enthalpy-temperature curves obtained by differential scanning calorimetry with a DSC, scanned at a constant heating rates of 2, 5, 10 and 15 °C/min. (2) Two kinetic models were used here: (i) empirical and (ii) phenomenological, in which the diffusional effect was incorporated in both models. The Kissinger method enabled the estimation of the activation energy values of the empirical model. The experimental curves were compared with the curing profiles calculated by using the kinetic parameters obtained with the minimization of the Euclidian norm of fitting error. (3) A typical pultrusion process was simulated by the use of the the Ansys CFX software with the incorporation of the proposed kinetic models. Curing and temperature profiles were analysed. The following conclusions are worth noting:

(i) The curing profiles allowed conclude that the inclusion of the diffusional term allowed to improve the estimation of the kinetic parameters considerably, presenting an average objective function and objective function reduction of 1.73 and 16.13%,

respectively, in relation to the results obtained with the non-diffusional empirical model.

(ii) The phenomenological model allowed to obtain an average objective function of 11.31% in relation to the results obtained with the diffusional empirical model, suggesting that the model is adequate to predict the curing reaction of the system.

(iii) The results of the simulation of pultrusion process revealed that both models presented a similar curing and temperature profiles. This indicates that the phenomenological model may also be an promising approach to be implemented for analysis.

For future implementations, we suggest the validation of simulated results by comparison with experimental data obtained from a pultrusion experiment.

8. References

[1] William D. Callister, David G. Rethwisch, Materials Science and Engineering: An
Introduction, John Wiley & Sons, 8th Edition, 2009.

[2] T. Sinmazcelik, E. Avcu, M. Ö. Bora, O. Coban, A rewiew: fibre metal laminates, backgraund types and applied test methods, Materials & Design 32 (2011) 3671–3685.

[3] D. F. Kersting, 2004, 'Evaluation of epoxy resins for the manufacture of composite materials by pultrusion process', Dissertation, Universidade Federal do Rio Grande do Sul, Porto Alegre, Brazil.

[4] EPTA European Pultrusion Technology Association AVK: World Pultrusion conference 2018, Imperial College, Viena, Austria, 1-2 March 2018.
https://www.lucintel.com/news/epta-highlights-prospects-for-pultruded-composites-in-infrastructure.aspx

[5] R. C. Dias, L. S. Santos, H. Ouzia, R. Schledjewski, Improving degree of cure in pultrusion process by optimizing die temperature. Materials Today communications, 17, pp. 362-370, 2018.

[6] R. C. Dias, L. S. Santos, H. Ouzia, R. Schledjewski, Comparative Study of Optimization in Pultrusion with Pre-Heating and Die-Cooler Temperature for Improved Cure. Materials Science Forum, 879, pp. 402-407, 2017

[7] R. C. Dias, L. S. Santos, H. Ouzia, R. Schledjewski, Optimization of die-temperature in pultrusion of thermosetting composites for improved cure, In: International Conference on Swarm Intelligence Based Optimization – Theoretical advances and real world application, Mulhouse, France, 13 – 14th June, 2016

[8] R. C. Dias, L. S. Santos, H. Ouzia, R. Schledjewski, Improved cure simulation in pultrusion process about heating systems: A case study, In: 17th European conference on composite materials ECCM17, Munich, Germany, 26 – 30th June, 2016.

[9] C. Dispenza, A. A. Pisano, P. Fuschi. Numerical simulations of mechanical characteristics of glass fiber reinforced C-profiles, Composite Science and Technology, 68 (2006) 47-56.

[10] ALMACO - Brazilian Association of Composite Materials.
http://almaco.org.br/noticias-2/

[11] F. J. G. Silva, F. Ferreira, M. C. S. Ribeiro, A. C. M. Castro, M. R. A. Castro, M. L. Dinis, A. Fiuza, Optimising the energy consumption on pultrusion process, Composites Part B: Engineering 57 (2014) 13–20.

[12] Lee L J, Young W B, Lin R J. Mold filling and cure modeling of RTM and SRIM processes. Composite Structures 27 (1994) 109-120.

[13] Stroller, R.G.; Modeling and thermal simulation of the pultrusion process. Dissertation (Master in Aeronautical and Mechanical Engineering) - Technological Institute of Aeronautics, São José dos Campos, 2005.

[14] Suratno, B.R., LIN, Y., Mai, Y.W. Simulation of temperature and curing profiles in pultruded composites rods. Composite Science and Technology, 58 (1998) 191-197.

[15] Nassem Arar, 2014, Production of Epoxy/E-glass composites using “clean Pultrusion”, Master thesis, School of Metallurgy and Materials College of Engineering and Physical Sciences University of Birmingham, United Kingdom.

[16] EPTA – European Pultrusion Techology Association. http://pultruders.com.

[17] Advani and Hsiao, Manufacturing techniques for polymer matrix composites (PMSc), 2012.

[18] Ismet Baran, 2014, ‘Modelling the Pultrusion Process of Off Shore Wind Turbine Blades’, PhD thesis, Technical University of Denmark, Denmark.

[19] Shape CORP. https://www.shapecorp.com/manufacturing/composites/

[20] Munmaya Mishra, Encyclopedia of polymer applications, 2019.

[21] Unicomposite. http://www.unicomposite.com/

[22] Swaraj Paul, Crosslinking: Chemistry of Surface Coatings, Comprehensive Polymer Science and Supplements 6 (1989) 149-192.

[23] Johannes Karl Fink, Reactive Polymers: Fundamentals and Applications. A Concise Guide to industrial Polymers, Third Edition (2018).

[24] Starr, Trevor F. Pultrusion for engineers. CRC Press. Cambrigde. England. 2000.

[25] J. Zhang, Y. C. Xu, P. Huang, Effect of cure cycle on curing process and hardness for epoxy resin, Express Polymer Letters 3 (9) (2009) 534-541.

[26] L.S. Santos, R. L. Pagano, V. M. A. Calado, E. Biscaia Jr., Optimization of a pultrusion process using finite difference and particle swarm algorithms, Brazilian Journal of Chemical Engineering 32 (2015) 543-553.

[27] V. Botelho, I. de Souza Moreira, J. O. Trierweiler, G. A. Neumann, M. Farenzena, Estimation of kinetic parameters of a polymerization reactor using real data, IFAC Proceedings Volumes 45 (2012) 685–690.

[28] M. N. Siddiqui, E. V. Antonakou, H. H. Redhwi, D. S. Achilias, Kinetic analysis of thermal and catalytic degradation of polymers found in waste electric and electronic equipment, Thermochimica Acta 675 (2019) 69–76.

[29] R. L. Pagano, V. M. Calado, F. W. Tavares, E. C. Biscaia, Cure kinetic parameter estimation of thermosetting resins with isothermal data by using particle swarm optimization, European Polymer Journal 44 (2008) 2678-2686.
[30] R. R. Corsetti, T. Neumeyer, M. May, D. Jandrey, V. Altstaedt, N. S. M. Cardozo, Modeling and estimation of parameters for the curing of an epoxy/amine system, Polymer Testing 32 (4) (2013) 647–654.

[31] S. Farahani, M. Sefidgar, F. Kowsary, Estimation of kinetic parameters of composite materials during the cure process by using wavelet transform and mollification method, International Communications in Heat and Mass Transfer 38 (2011) 1305–1311.

[32] B. Janković, The kinetic analysis of isothermal curing reaction of an un saturated polyester resin: Estimation of the density distribution function of the apparent activation energy, Chemical Engineering Journal 162 (2010) 331–340.

[33] R. de P. Soares, A. Secchi, EMSO: A new environment for modelling, simulation and optimisation, in: Computer Aided Chemical Engineering, Elsevier, 2003, pp. 947–952.

[34] N. Sbirrazzuoli, S. Vyazovkin, Learning about epoxy cure mechanisms from isoconversional analysis of DSC data, Thermochimica Acta 388 (1-2) (2002) 289–298.

[35] M. R. Kamal, S. Sourour, Kinetics and thermal characterization of thermoset cure, Polymer Engineering and Science 13 (1973) 59–64.

[36] S. Du, Z.-S. Guo, B. Zhang, Z. Wu, Cure kinetics of epoxy resin used for advanced composites, Polymer International 53 (2004) 1343–1347.

[37] M. Javdanitehran, D. C. Berg, E. Duemichen, G. Ziegmann, An iterative approach for isothermal curing kinetics modelling of an epoxy resin system, Thermochimica Acta 623 (2016) 72–79.

[38] L. Matějka, J. Lövy, S. Pokorný, K. Bouchal, K. Dušek, Curing epoxy resins with anhydrides. Model reactions and reaction mechanism, Journal of Polymer Science: Polymer Chemistry Edition 21 (1983) 2873–2885.

[39] L. Granado, S. Kempa, L. J. Gregoriades, F. Brüning, A. C. Genix, N. Frétyc, E. Anglaret, Kinetic regimes in the curing process of epoxy phenol composites, Thermochimica Acta 667 (2018) 185–192.

[40] L. Matějka, J. Lövy, S. Pokorný, K. Bouchal, K. Dušek, Curing epoxy resins with anhydrides. Model reactions and reaction mechanism, Journal of Polymer Science: Polymer Chemistry Edition 21 (1983) 2873–2885.

[41] M. Pham, Theoretical Studies of Mechanisms of Epoxy Curing Systems, Ph.D. thesis, The University of Utah (2011).

[42] M. R. Saeb, E. Bakhshandeh, H. A. Khonakdar, E. Mäder, C. Scheffler, G. Heinrich, Cure Kinetics of Epoxy Nanocomposites Affected by MWCNTs Functionalization: A Review, The Scientific World Journal (2013) 1–14.

[43] L. R. Amirova, A. R. Burilov, L. M. Amirova, I. Bauer, W. D. Habicher, Kinetics and mechanistic investigation of epoxy-anhydride compositions cured with quaternary phosphonium salts as accelerators, Journal of Polymer Science, Part A: Polymer Chemistry 54 (2016) 1088–1097.

[44] M. K. Antoon, J. L. Koenig, Crosslinking mechanism of an anhydride-cured epoxy resin as studied by fourier transform infrared spectroscopy, Journal of Polymer Science: Polymer Chemistry Edition 19 (1981) 549–570.

[45] R. M. L. Coelho, V. M. A. Calado, An optimization procedure for the pultrusion process based on a finite element formulation, Polymer Composites 23 (2002) 329-334.

[46] S. C. Joshi, Y. C. Lam, Three-dimensional finite-element/nodal-control volume simulation of the pultrusion process with temperature-dependent material properties including resin shrinkage, Composites Science and Technology 61 (2001) 1539-1547.

[47] D. Srinivasagupta, J. L. Kardos, B. Joseph, Rigorous dynamic model-based economic design of the injected pultrusion process with controllability considerations, Journal of Composite Materials 37 (2003) 1851–1880.

[48] P. Carlone, G. S. Palazzo, R. Pasquino, Pultrusion manufacturing process development by computational modelling and methods, Mathematical and Computer Modelling 44 (2006) 701–709.

[49] L. S. Santos, R. L. Pagano, E. C. Biscaia, V. M. A. Calado, Optimum heating configuration of pultrusion process, in: Computer Aided Chemical Engineering, Elsevier, (2009) 705–710.

[50] F. J. G. Silva, F. Ferreira, M. C. S. Ribeiro, A. C. M. Castro, M. R. A. Castro, M. L. Dinis, A. Fiuza, Optimising the energy consumption on pultrusion process, Composites Part B: Engineering 57 (2014) 13–20.

[51] I. Baran, J. H. Hattel, R. Akkerman, Investigation of process induced warpage for pultrusion of a rectangular hollow profile, Composites Part B: Engineering 68 (2015) 365–374.

[52] A. A. Safonov, P. Carlone, I. Akhatov, Mathematical simulation of pul-trusion processes: A review, Composite Structures 184 (2018) 153-177.

[53] Akishin P, Barkanov E, Bondarchuk A, Finite Element Modelling and Analysis of Conventional Pultrusion Processes, IOP Conference Series: Materials Science and Engineering (2015).

[54] Liszka T, Orkisz J, The finite difference method at arbitrary irregular grids and its application in applied mechanics. Computers and Structures 11 (1980) 83-95.

[55] Hidajet Hadzic, Development and Application of a Finite Volume Method for the Computation of Flows Around Moving Bodies on Unstructured, Overlapping Grids. Ph.D. thesis, Technischen Universität Hamburg-Harburg (2005).

[56] Moukalled F, Mangani L, Darwish M, The Finite Volume Method in Computational Fluid Dynamics, Fluid mechanics and its Applications (1980).
[57] Jeferson Avila Souza, 2000, Implementation of a Method of Finite Volumes with local coordinate system for the coupled soulution of navier-stoke equations, Dissertation, Federal University of Santa Catarina, Florianópolis.

[58] L. Calabrese, A. Valenza, The effect of a liquid CTBN rubber modifier on the thermo-kinetic parameters of an epoxy resin during a pultrusion process, Composites Science and Technology 63 (2003) 851-860.

[59] S.C. Joshi, Y. Lam, U. Win Tun, Improved cure optimization in pultrusion with pre-heating and die-cooler temperature, Composites Part A: Applied Science and Manufacturing 34 (2003) 1151-1159.

[60] R. Poli, J. Kennedy, T. Blackwell, Particle swarm optimization, Swarm Intelligence 1 (2007) 33-57.

[61] I.C. Trelea, The particle swarm optimization algorithm: convergence analysis and parameter selection, information Processing Letters 85 (2003).

[62] J. Li, S. C. Joshi, Y. Lam, Curing optimization for pultruded composite sections, Composites Science and Technology 62 (2002) 457-467.

[63] L. Su, L. Tang, D. E. Bernal, I. E. Grossmann, Improved quadratic cuts for convex mixed-integer nonlinear programs, Computers & Chemical Engineering 109 (2018) 77-95.

[64] W. W. Hager, J. T. Hungerford, Continuous quadratic programming formulations of optimization problems on graphs. European Journal of Operational Research 240 (2015) 328-337.

[65] A. Khodabakhshian, M. P. Ezatabadi, R. Hooshmand. Design of a robust load frequency control using sequential quadratic programming technique. ElectPower Energy Syst 40 (2012) 1–8.

[66] S. Corezzi, D. Fioretto, G. Santucci, J. M. Kenny, Modeling diffusion control in the cure kinetics of epoxy-amine thermoset resins: An approach based on configurational entropy, Polymer 51 (2010) 5833–5845.

[67] R.R. Corsetti, T. Neumeyer, M. May, D. Jandrey, V. Altstaedt, N. S. M. Cardozo, Modeling and estimation of parameters for the curing of an epoxy/amine system, Polymer Testing 32 (2013) 647-654.

[68] R. L. Pagano, V. M. Calado, F. W. Tavares, E. C. Biscaia, Cure kinetic parameter estimation of thermosetting resins with isothermal data by using particle swarm optimization, European Polymer Journal 44 (2008).

[69] Ricky Hardis, 2012, Cure kinetics characterization and monitoring of an epoxy resin for thick composite structures, PhD thesis, Iowa State University, Ames, Iowa.

[70] H. E. Kissinger, Reaction kinetics in differential thermal analysis, Analytical Chemistry 29 (11) (1957) 1702-1706.

[71] A. Bernath, L. Krger, F. Henning, Accurate cure modeling for isothermal processing of fast curing epoxy resins, Polymers 8 (11) (2016) 390.

[72] R. L. Blaine, H. E. Kissinger, Homer Kissinger and the Kissinger equation, Thermochimica Acta 540 (2012).

[73] S. Mardle, K. M. Miettinem, Nonlinear Multiobjective Optimization, Vol. 51, 2006.

[74] L. S. Santos, E. C. B. Jr., R. L. Pagano, V. M. A. Calado, CFD-optimization algorithm to optimize the energy transport in pultruded polymer composites, Brazilian Journal of Chemical Engineering 29 (3) (2012).

[75] J.W. Vergnaud, J.Bouzon, Cure of Thermosetting Resins, 2011.

[76] V. Botelho, I. de Souza Moreira, J. O. Trierweiler, G. A. Neumann, M. Farenzena, Estimation of kinetic parameters of a polymerization reactor using real data, IFAC Proceedings Volumes 45 (2012) 685-690.

9. Appendix

Optimization Routine – Optimizing die-heating in pultrusion thermoseting Composites the Pultrusion function.

Let us consider the following function:

$$F(x) = \sum_{j=1}^{n} (\sum_{i=1}^{m} \alpha_{ij} x_i + b_j)^2,$$

where:

m and *n* are two nonnegative integers.

A=(α_{ij}) is a *m* x *n* matrix. For any index j, α_j will denote the *j-th* column of the matrix A.

b is an *n* – vector

The function ***F*** can be rewritten as follows:

$$F(x) = \frac{1}{2} x^t H x + v^t x + w$$

where:

H is semi-definite matrix such that: $H = 2\sum_{j=1}^{n} a_j \alpha_j^t$

v is defined as follows $v = 2\sum_{j=1}^{n} 2b_j \alpha_j^t$,

w is the Euclidian norm of the vector b.

Control parameters

The following control variables are necessary for the later purposes.

```
clc;
clear all;

teste()
%---
%--- FILENAME
%---
ampldatadir  = '../../data/';
amplfilename = 'ampl-data.dat';

%csvdir       = '../../csv/06/17/';
%csvfilename  = 'iter-0.csv';

csvdir = 'C:\Users\RITA\Documents\MATLAB\projeto\data\';
csvfilename = 'csv 6-6-2016-T177-SP2.99-Int1-A.csv';

soldir       = csvdir;
solfilename  = strcat('sol-',csvfilename);
solfilename  = strcat(solfilename,'.txt');

%---
%--- CONTROL VARIABLES
%---

 LOAD_FROM_FILE     = true;
 EXPORT_AMPL_DATA   = false;
 EXPORT_SOLUTION    = true;

 HEAT_UNIT_CHANGE   = 10; % [k]
 ALPHA_DESIRED      = 0.9;

 %---
 %---DATA
 %---
 if LOAD_FROM_FILE
     %---
     %--- DATA FROM FILE
     %---
     filename = strcat(csvdir,csvfilename);
     [A,b] =
PultfuncImportParams(filename,HEAT_UNIT_CHANGE,ALPHA_DESIRED);
     [M,N] = size(A);
 else
     %---
     %--- RANDOM DATA
     %---
     M = 15;             % Nbr rows of the matrix A
     N = 100;            % Nbr cols of the matrix A
     A = rand(M,N);      % A random matrix A
     b = rand(1,N);      % A rondom vector b
 end

 %---
 %---INITIAL VALUES
 %---

 T0 = 490*ones(M,1);
```

```
 Tmax = 500* ones(M,1); % Upper bound suggested


 [H,v,w] = PultfuncGetQform(A,b);
 % [VALPROP,VECPROP] = eig(H)
 %
 % det(VECPROP)
 % error('stop: just ca...') ;

 %--- ASSERT:
 %--- The functios Pultrusions PultfuncQform(...) and Pultfunc
 %--- must return the same values.
 %---
 x = ones(M,1);
 Pultfunceval = Pultfunc(x,A,b);
 PultfuncevalBis = PultfuncQform(x,H,v,w);

 DT= (Tmax-T0);
 %DT = 278.15 * ones(nbrHeaters,1) % Initial values used in J. Li et al
                                   % what can be the effect of using
                                   % different values for DT ? For
example
                                   % using DT=Tmax-T0

 lb = -DT;
 ub = DT;

 if EXPORT_AMPL_DATA
     filename = strcat(ampldatadir,amplfilename);
     PultfuncAmplExport(filename,M,N,A,b,lb,ub);
 end

 func = @(x) Pultfunc(x,A,b);
 nvars = M;
 options = optimoptions('particleswarm','Swarmsize',100);
 %options.HybridFcn = @fmincon;
 [psosol,psoval] = particleswarm(func,nvars,lb,ub,options);

 %%[sol,objval,exitflag,output] = fmincon(Psosol,[],[],[],[],lb,ub;

 %xstart = psosol;%zeros(nbrHeaters,1);%
 options = optimoptions('quadprog','Algorithm','trust-region-
reflective');
 [quadsol,quadval] = quadprog(H,v,[],[],[],[],lb,ub,[],options);

 %[cpxsol,cpxval,exitflag,output] = cplexqp(H,v,[],[],[],[],lb,ub);
 cpxsol = quadsol;
 cpxval = quadval;

 filename = strcat(soldir,solfilename);


PultfuncOutputs(EXPORT_SOLUTION,filename,nvars,w,T0,lb,ub,psosol,quadsol,
cpxsol,psoval,quadval,cpxval)
```

```
function rval = Pultfunc(x,A,b)

%
% USAGE
%  rval = Pultval(X,A,b);
%
% INPUTS:
%   x = vector of size m: (temperatur, speed)
%   A = Matrix of size mxn: degree of cure (for each control volume)
%   b = vector of size n:
%
% OUTPUT:
% rval: the value of the Pultrusion function in the point x
%

[nbrRows, nbrCols] = size(A);
sizeb = size(b);
if sizeb ~= nbrCols
    error(' Dimension mismatch: the number of columns of the matrix A is
not equal the size of the vector b. ');
end

rval = 0;
for j=1:nbrCols
    temp = 0;
    for i=1:nbrRows
        temp = temp + A(i,j)*x(i);
    end
    rval = rval + (temp+b(j))^2;
end
end



function [H,v,w] = PultfuncGetQform(A,b)
%
% USAGE:
%   [H,v,w] = qformPultfunc(A,b)
% INPUTS:
%   A: an mxn-Matrix (related to the degree of cure)
%   b: an m-vector
%
% OUTPUT:
%   H: the mxm-hessian matrix of the quadratic form
%   v: the m-vector of the linear part
%   w: the constant

[nbrRows, nbrCols] = size(A);
sizeb = size(b);

if sizeb ~= nbrCols
    error(' Dimension mismatch: nbrcols(A) not equal to size(b). ');
end

% The matrix H of size : mxm
H = zeros(nbrRows,nbrRows);
for j=1:nbrCols
```

```
    H = H + A(:,j)*transpose(A(:,j));
end
H = 2*H;

% The vector v
v = zeros(nbrRows,1);
for j=1:nbrCols
    v = v + 2*b(j)*A(:,j);
end

% the constant w
w = 0;
for j=1:nbrCols
    w = w + b(j)*b(j);
end
end
```

```
function [A,b] = PultfuncImportParams(filename,DHeat,DOCDesired)
    disp('nome do aquivo:');
    disp(filename);
%
% USAGE:
% [Matrix,Vector] = PultfuncImportParams(filename,DHeat,DOCDesired)
%
% INPUT:
% filrname: the file from where to read the data
% DHeat: Used die heater inite change
% DOCDesired: Desired degree of cure
%
% FILE FORMAT:
% columns: refval valHeater1 valHeater2 ....
% delimiter: ,

data = dlmread (filename,','); % nbrElements x (1+nbrHeaters)
[nbelems,nbcols] = size(data);
nvars = nbcols - 1;

b = zeros(nbelems,1);
b = data(:,1) - DOCDesired;

M = zeros(nbelems,nvars);

for k=2:nbcols
    M(:,k-1) = (1/DHeat).*(data(:,k) - data(:,1));
end

A = transpose(M);
end
```

```
function PultfuncOutputs(EXPORT_SOLUTION,
filename,nvars,w,T0,lb,ub,psosol,quadsol,cpxsol,psoval,quadval,cpxval)
%
% USAGE:
%   PultfuncOutputs
%
% INPUTS:
%   EXPORT_SOLUTION: If true then exports the data to an AMPL format
%          filename: where to export the AMPL data
%             nvars: Number of variables (temperature and pull-speed)
%                 w: constant to add to the quadval and cpxval
%                T0: The inicial temperature
%                lb: Lower bound
%                ub: Upper bound
%            psosol: PSO solution
%           quadsol: QP solution
%            cpxsol: CPX solution
%            psoval: PSO solution value
%           quadval: QP solution value
%            cpxval: CPX solution value
%
%---
%--- PRINT OUT SOLUTION FOUND
%---

fprintf('+----------------------\n');
fprintf('+ Solution found by each solver\n');
fprintf('+\n');
fprintf('\n\n');
fprintf('%4s %8s %8s %8s %8s %8s\n', 'vars','lb','ub', 'Pso',
'QP','CPX');
for k=1:nvars
    fprintf('%4d %8.2f %8.2f %8.2f \n', k,lb(k), ub(k), psosol(k),
quadsol (k),cpxsol(k));
end
fprintf('\r\n%4s %8s %8s %8s.2f %8.2f %8.2f \n', 'objv.','-','-', psoval,
quadval+w,cpxval+w);
fprintf('\n\n');

%---
%--- COMPUTE THE NEW SETTING
%---

PSOTemp = zeros(nvars,1);
QPTemp  = zeros(nvars,1);
CPXTemp = zeros(nvars,1);
for k=1:nvars
    PSOTemp(k) = psosol(k)+T0(k);
    QPTemp(k)  = quadsol(k)+T0(k);
    CPXTemp(k) = cpxsol(k)+T0(k);
end

%---
%---PRINT OUT THE NEW TEMPERATURES
%---

fprintf('---------------------------------\n');
fprintf('+ New set of heating temperatures [k]\n');
```

```
fprintf('+\n');
fprintf('\n\n');
fprintf('%7s %8s %8s %8s %8s\n', 'Heater','T0','Pso','QP','CPX');
for k=1:nvars
    fprintf('%7d %8.2f %8.2f %8.2f %8.2f \n',
k,T0(k),PSOTemp(k),QPTemp(k),CPXTemp(k));
end

%---
%--- EXPORT RESULTS TO FILE
%---

if EXPORT_SOLUTION
    fileid = fopen(filename,'w');
    fprintf(fileid,'+ New set of heatting temperatures [k]\n');
    fprintf(fileid,'+ \n');

    fprintf(fileid,'\n\n');
    fprintf(fileid,'%7s %8s %8s %8s %8s\n',
'Heater','T0','Pso','QP','CPX');
    for k=1:nvars
        fprintf(fileid,'%7d %8.2f %8.2f %8.2f %8.2f \n',
k,T0(k),PSOTemp(k),QPTemp(k),CPXTemp(k));
    end
end
%---
%--- END
%---
fprintf('\n\n');
fprintf('+-------- THE END');
end
 function eval = PultfuncQform(x,H,v,w)
    %
    % USAGE:
    %  eval: PultfuncQform(x,H,v,w)
    %
    % INPUTS:
    % x:
    % H:
    % v:
    % w:
    %
    % OUTPUT:
    %

    eval = 0.5*transpose(x)*H*x + transpose(v)*x + w;
end
```

Optimization Routine - Kinetic model

```
global T
global data

load('T10.dat');
load('data10.dat');
```

```
T = T10;
data = data10;

x0 = [2; 7];      % Make a starting guess at the solution
% x0 = [0.304289728807862;0.0124172676155399;10000]
x = [3 849704.719191115];
x = [2.2496  298.730000 0.01]
% options_s = optimoptions('particleswarm','SwarmSize',2, 'Display',
'iter', 'MaxIter', 30 );
% [x,fval,exitflag] = particleswarm(@objfun,2,[0.00001 1e3],[3
1e8],options_s);

options = optimoptions(@fmincon,'Algorithm','interior-point', 'Display',
'iter');
[x,fval] = fmincon(@objfun,x,[],[],[], [],[0.00001 1e-5 0 ],[3 1e8 5
0.05],[],options);

function obj = objfun(N)
global T
global data

%  N = [1.21027667913748 459497.891714916]; % Method 1
% N =  [[0.553405316808172 999999.986778218]]; % Method 2
% N = [2.09388701647617 548570.738908493];
% N = [0.587889059488007 426577.436126345]
% N = [0.621456618418210 1973952.91717915];
ko = 118;
Ao = 0.0;
% n = N(1) + N(3)*T;
ke = N(2);
Yo = [];
% Ea = N(3);
kmax = length(T);
for k=1:kmax
tspan=linspace(ko,ko+1,3);
[time,Y] = ode45(@(t,y)rigid(t,Ao,N,ke,T(k)),tspan,Ao);
ko = ko+1;
Yo = [Yo; Y(end)];
Ao = Y(end);
end

function dy = rigid(t,y,N,ke,T)

Ea = 63.717*1e3; %kJ/mol % Method 1

% Ea = 68.785*1e3; %kJ/mol % Method 2
% m=0;
R = 8.314; %J/mol/K
T = T+273.15;
n = N(1) + N(3)*T;
dy = ke*(exp(-Ea/(R*T)))*(1-y)^(n);

end
```